KINETIC STUDY OF HISTIDINE KINASE CheA IN BACTERIAL CHEMOTAXIS

A Dissertation

presented to

the Faculty of the Graduate School

at the University of Missouri-Columbia

In Partial Fulfillment

of the Requirements for the Degree

Doctor of Philosophy

---

by

WENLIN PAN

Dr. Gerald Hazelbauer, Dissertation Supervisor

July 2017

The undersigned, appointed by the dean of the Graduate School, have examined the dissertation entitled

KINETIC STUDY OF HISTIDINE KINASE

CHEA IN BACTERIAL CHEMOTAXIS

presented by Wenlin Pan,

a candidate for the degree of doctor of philosophy,

and hereby certify that, in their opinion, it is worthy of acceptance.

Professor Gerald Hazelbauer

Professor Linda Randall

Professor Peter Tipton

Professor Pamela Brown

Professor John Tanner

ACKNOWLEDGEMENTS

I am grateful to my advisor, Dr. Gerald Hazelbauer, whose expertise and wisdom have guided me along the way for a successful completion of my doctorate degree. I thank him for being patient and supportive through the entire process. I enjoyed working with him.

I would like to express my gratitude to Dr. Linda Randall for providing valuable comments and suggestions on my work during group meetings. I appreciate her encouragement after each of my presentation.

I thank my other committee members, Peter Tipton, Pamela Brown, and Jack Tanner for their help and contributions.

I am thankful to Mingshan Li for being a lab mentor who is always responsive and helpful when I have questions regarding to lab experiments and computer software.

I would like to thank Wing-Cheung Lai, Chunfeng Mao, Priya Bariya, Yuying Suo, Narahari Akkaladevi and Angela Lilly for their help and advice and for creating a warm lab environment.

I would like to acknowledge former lab members Nicholas Bartelli and Bahar Tuba Findik for their help and kindness.

I would like to express my gratitude to our "lab mother" Mary Belle Streit for taking care of the lab and preparing tea and snacks during "tea time" and for spreading warmth and kindness to everybody.

I thank our collaborator Frederick Dahlquist for his original idea on this project and contributions of his thoughts and experimental materials along the process.

I thank my parents for going through all the troubles raising me up.

TABLE OF CONTENTS

LIST OF FIGURES

LIST OF TABLES

Kinetic study of histidine kinase CheA in bacterial chemotaxis

Wenlin Pan

Dr. Gerald Hazelbauer, dissertation advisor

ABSTRACT

Histidine kinase CheA is central to signaling in bacterial chemotaxis. This kinase is responsible for the phosphorylation of two response regulators, CheY and CheB. CheY controls flagellar rotation and thus motility. CheB is crucial for sensory adaptation. CheA is dramatically activated, up to 1000-fold, and put under the control of chemoreceptors by formation of the signaling complex. As measured by phosphorylation of CheY, this control modulates the activity of CheA in a range as wide as two orders of magnitude. This change in the activity of CheA is the essence of chemotactic signaling. However, the enzymatic properties altered by kinase incorporation into signaling complexes, chemoreceptor ligand binding or receptor adaptational modification are largely undefined. This dissertation describes the kinetic analysis of kinase CheA. Data are fit to the Michaelis-Menten equation, from which important parameters K_M and k_{cat} are obtained. Based on these parameters for CheA at different signaling conditions, important observations and conclusions are made to contribute to better understanding of the control of the activity of kinase CheA, thus the bacterial chemotaxis signaling system.

CHAPTER ONE

Bacteria chemotaxis and key proteins

Bacteria chemotaxis

Chemotaxis is the ability of bacteria to get to favorable places where the nutrients are abundant but the toxins are sparse (Wadhams & Armitage, 2004; Hazelbauer et al., 2008; Hazelbauer & Lai, 2010; Sourjik & Wingreen, 2012; Parkinson et al., 2015). In *Escherichia coli*, this crucial skill is fulfilled by controlling the rotation direction of the flagella on their bodies. The flagellar rotary motor, driven by proton-motive force (Manson et al., 1977), is set to rotate counter-clockwise (CCW), causing the flagella to bundle, thus the cell swims forward in one direction (run) (Berg, 2000). Occasionally, the flagellar rotary motor rotates clockwise (CW) (Eisenbach, 1996), which temporally dissociates the flagella bundle (Berg, 2000). The cell then stops and picks up a new running direction randomly (tumble). Therefore, in solution, bacterial cells trace a random walk (Berg, 2000). This random walk is biased towards the highest in a concentration gradient generated by attractants (Berg, 2000). How do bacteria "know" when to run and when to tumble? It all relies on the "brain" of bacteria—the chemotaxis signaling system.

Bacterial two-component signaling system

Unlike most eukaryotic signaling pathways that rely on serine, threonine or tyrosine kinases, bacterial signaling depends heavily on a histidine-aspartate phosphorelay system, namely two-component signaling system (TCS) (Fig. 1) (Bourret et al., 1989; Falke et al., 1997; Bren & Eisenbach, 2000; Stock et al., 2000).

The first component, a sensor histidine protein kinase together with its cognate response regulator, the second component, are widely used across almost all bacterial species

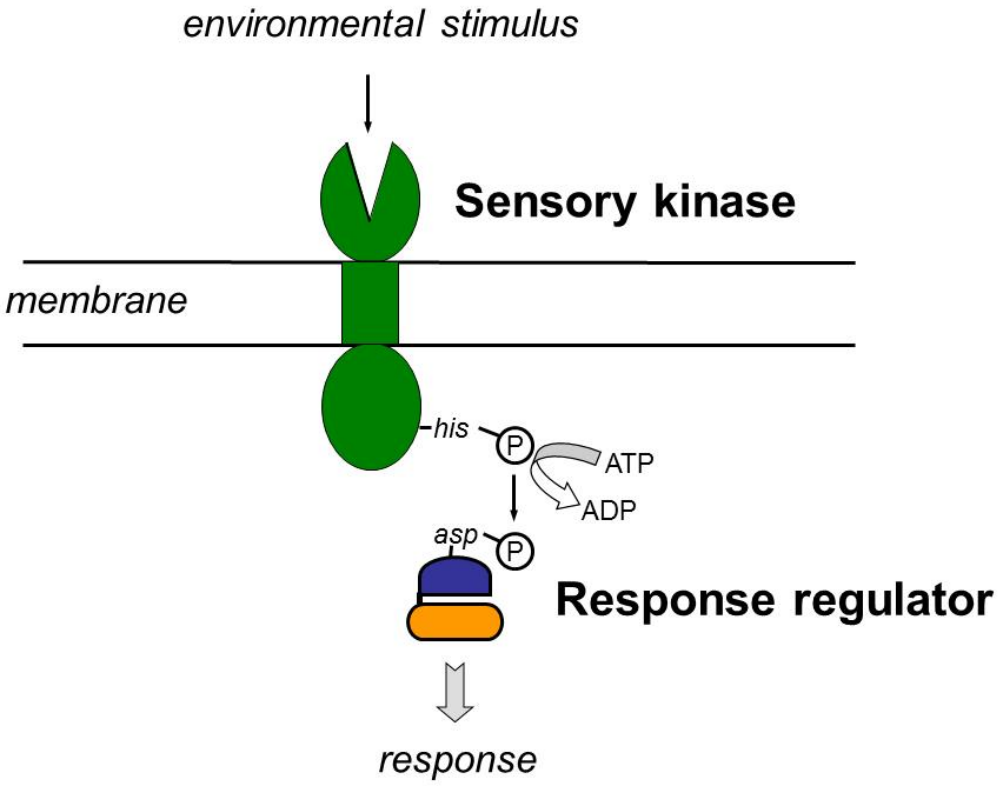

Fig. 1. Cartoon representing the two-component signaling system. The first component, a sensory kinase is represented in green with its periplasmic sensor domain, transmembrane domain and cytoplasmic domain shown in different shapes. The second component, a response regulator, often a transcriptional effector (Gao & Stock, 2009), has two domains, with the receiver domain that carries the Asp residue in blue and the effector domain that usually binds to DNA in orange.

(Wolanin et al., 2002). There are over a thousand histidine protein kinase genes that have been sequenced, some of which exist in archaea and lower eukaryotes, but with much less frequency than in bacteria (Wolanin et al., 2002). Histidine kinases are not found in higher eukaryotes where Ser, Thr and Tyr kinases are dominant in signaling transduction pathways. There are around 30 histidine kinases identified in *E. coli* (Dutta et al., 1999; West & Stock, 2001), which are used to respond to changes in the environment, such as temperature, light, salinity, oxygen and signaling molecules (Baker et al., 2006). Their ATP-binding catalytic domains share conserved sequence motifs N, G1, F and G2 boxes (regions that feature one or several asparagine, glycine, phenylalanine, glycine residues, respectively, responsible for binding ATP) (Parkinson & Kofoid, 1992; Swanson et al., 1994). They remain as active homodimers through the dimerization domains, each of which donates a two-stranded coiled-coil, forming a four-helix bundle structure (Stock & Surette, 1996; Dutta et al., 1999). With very few exceptions, the dimerization domain carries an H-box, another signature motif of histidine protein kinases (Parkinson & Kofoid, 1992; Swanson et al., 1994). The phosphor-receiver His in this H-box is autophosphorylated *in trans*, with the catalytic domain of one protomer phosphorylating the H-box His from the other protomer. There are two major classes of histidine kinases classified based on the position of the conserved histidine-containing region relative to the kinase region in their primary sequences (Bilwes et al., 1999). In class I histidine kinases, the H-box is on the same region as the N, G1, F and G2 boxes. However, in classs II histidine kinases, with CheA being the sole representative in *E. coli* (Dutta et al., 1999), the H-box is isolated in a different domain. Class I histidine kinases are often transmembrane receptors at the same time, with N-terminal periplamic sensing domains

that are variable in sequences, reflecting the different environmental signals that different histidine kinases respond to. On the other hand, CheA is a cytosolic histidine kinase that interacts with a distinct sensor transmembrane receptor through one of its domains with the help of a coupling protein.

The osmosensor EnvZ, a typical class I histidine kinase, has been studied extensively (Aiba & Mizuno, 1990; Park et al., 1998; Zhu et al., 2000). One monomer of EnvZ contains an N-terminal periplasmic sensing domain and a cytoplasmic histidine kinase region that is composed of two complimentary domains, the histidine-containing dimerization domain and a C-terminal ATP-binding catalytic domain. The NMR solution structures of the 67-residue dimerization domain (Tomomori et al., 1999) and the 161-residue catalytic domain (Tanaka et al., 1998) have been solved. The dimerization domain serves as the docking site at the bottom part of the four-helix bundle for the response regulator OmpR (Tomomori et al., 1999). The catalytic domains of EnvZ and CheA are structurally homologous. They also show striking homology to the ATP-binding domains of three ATPases, Hsp90 (Prodromou et al., 1997), DNA gyrase B (Wigley et al., 1991) and MutL (Ban & Yang, 1998), sharing a primarily 3α/4β sandwich structure (West & Stock, 2001).

Upon detection of stimuli by the periplasmic sensor, signal transduction occurs by autophosphorylating the His exposed at the four-helix bundle cytoplasmic domain. The phosphoryl group is then transferred to an Asp residue that is on the response regulator (Fig. 1), which changes its conformation, thus the affinity to its target, typically gene promoters (Gao & Stock, 2009). In addition to their kinase activity, many histidine kinases also have phosphatase activity towards cognate phosphorylated response

regulators (Gao & Stock, 2009). Thus all these reactions – autophosphorylation, phosphotransfer and phosphatase – are regulatory points during the signaling pathway.

CheA, the histidine kinase responsible for chemotaxis in *E. coli*, is localized in the cytosolic region. The signal of attractant binding is sensed by a distinct transmembrane receptor and transmitted to CheA, the activity of which is reduced as a result. Active CheA phosphorylates CheY and CheB, the response regulators. Once phosphorylated, CheY binds to the flagellar rotary motor, changing its default CCW rotation to CW (Eisenbach, 1996). Unlike class I histidine kinases, CheA is monofunctional with only kinase activity (Gao & Stock, 2009). Thus a separate phosphatase, CheZ, controls the cellular level of phosphorylated CheY (McEvoy et al., 1999). CheB together with another receptor modification enzyme, CheR, are responsible for the sensory adaptation mechanism that regulates the activity of CheA. CheR adds methyl groups donated by S-adenosylmethionine (SAM) to four glutamate residues on the cytoplasmic region of receptors, making them suitable for activating kinase CheA (Springer & Koshland, 1977). CheB, once phosphorylated by activated CheA, removes the methyl groups on those four modification sites, altering the receptors back to a kinase-off state (Kehry & Dahlquist, 1982; Kehry et al., 1985). The null state of signaling complex has an intermediate kinase activity. Methylation and demethylation drive the signaling complex to kinase-on and kinase-off states, respectively (Fig. 2). Thanks to this adaptation mechanism, bacteria can respond to changes in their environment across broad concentration ranges.

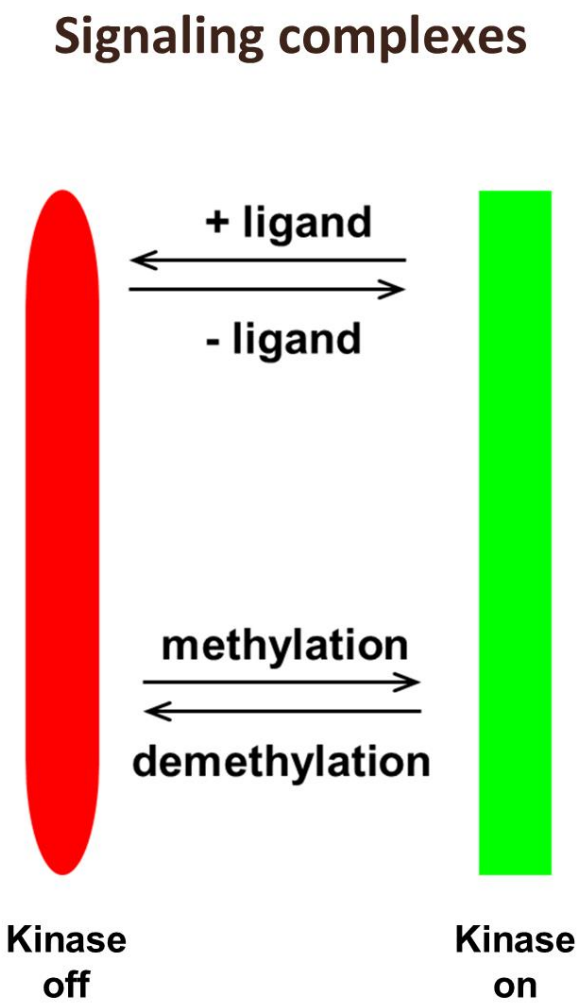

Fig. 2. The cycle between kinase-on and kinase-off signaling complexes affected by two allosteric effectors: ligand occupancy and receptor modification.

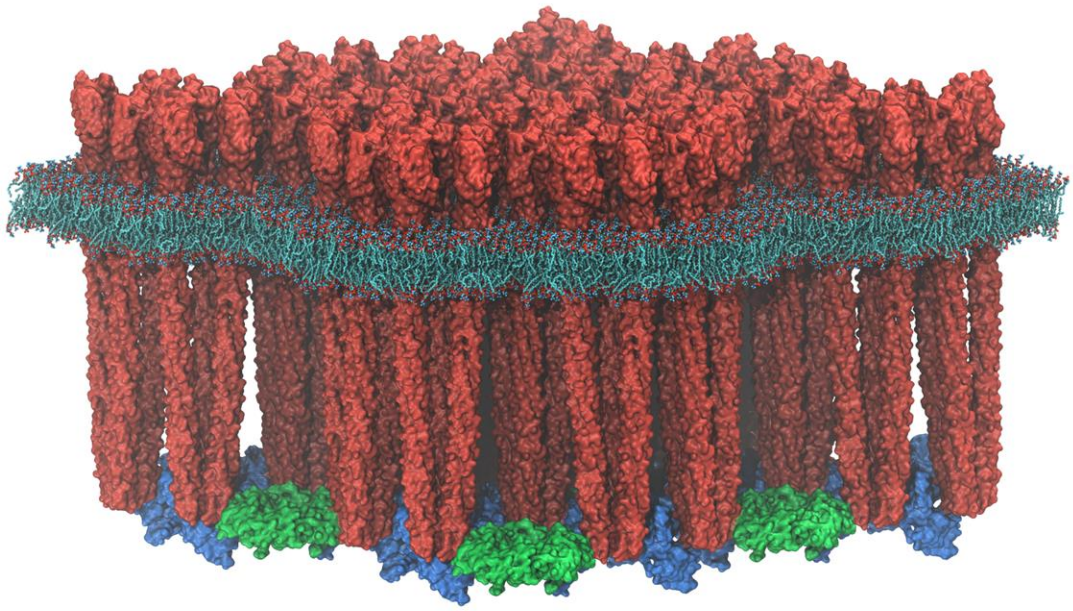

Fig. 3. Chemotaxis signaling complex array structure, adapted from (Goh et al., 2016). Transmembrane chemoreceptors are shown in red as trimers of dimers. CheW is shown in green. CheA is in blue.

Signaling complex

A marvelous protein architecture exists at the cell poles of *E. coli* (Briegel et al., 2012; Liu et al., 2012; Briegel et al., 2014). This is a structure made of thousands of proteins — receptors, CheW and CheA (Fig. 3). Looking down from the cytoplasmic membrane, it is an extension of many hexagonal arrays with the receptors being the six vertices (Briegel et al., 2012; Briegel et al., 2014). The tip of the receptors is the region that interacts with CheW and CheA. This interaction keeps the huge array structure together (Studdert & Parkinson, 2005; Erbse & Falke, 2009), enabling them to work cooperatively to process signals (Duke & Bray, 1999; Sourjik & Berg, 2002; Li & Hazelbauer, 2005). CheA is greatly activated in such a signaling complex and placed under control of receptors (Borkovich et al., 1989; Ninfa et al., 1991; Li & Hazelbauer, 2011a). Does signaling happen only with this huge array structure? Li and Hazelbauer (Li & Hazelbauer, 2011a) figured out the minimum copies of receptors, CheW and CheA to activate and control kinase activity — the core signaling complex (Fig. 4). Two trimers of receptor dimers, two copies of CheW and one CheA dimer make up this core signaling complex. It works as well as larger complexes in terms of activating and controlling the activity of kinase CheA (Li & Hazelbauer, 2011a).

Figure 5 shows the ribbon diagram of all the key proteins in bacterial chemotaxis and their interactions in a core signaling complex. The paragraphs in following sections discuss each protein in detail.

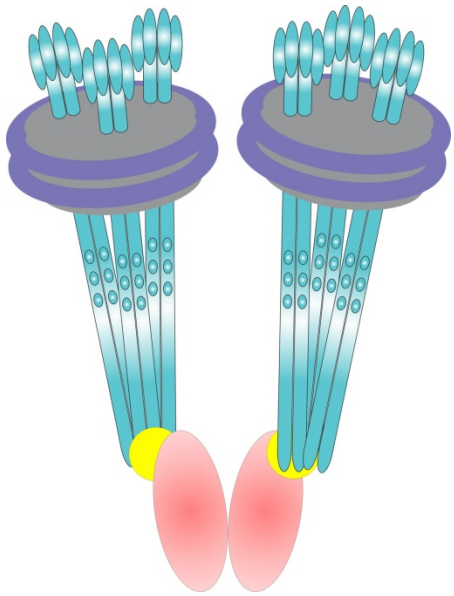

Fig. 4. Core signaling complex, adapted from Li & Hazelbauer's (Li & Hazelbauer, 2011a). Receptors embedded in Nanodiscs are shown in blue as trimers of dimers. Ovals on receptors represent their modification sites. Two copies of CheW are shown as yellow balls. CheA is in red as a dimer.

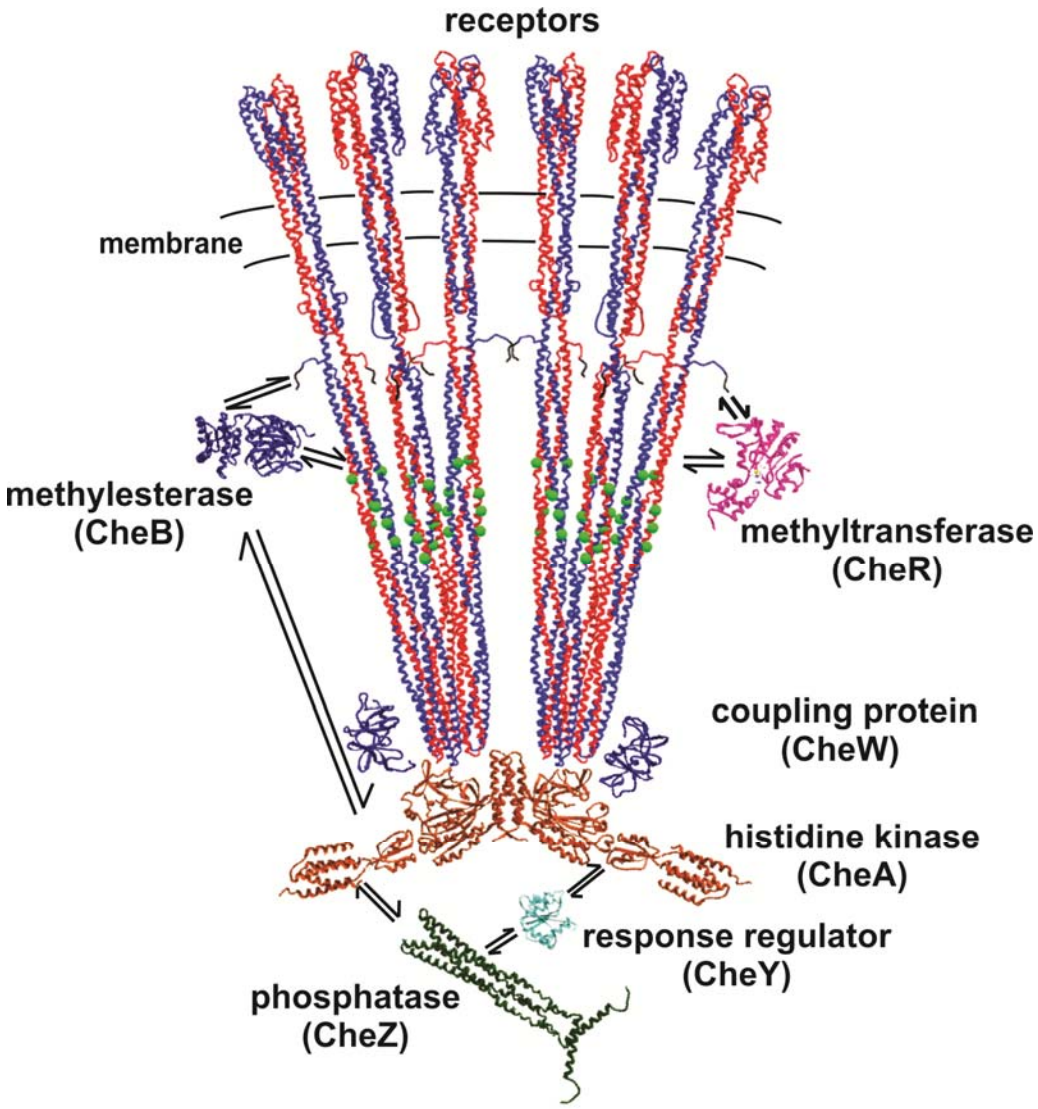

Fig. 5. Ribbon diagram of all the key proteins in the bacterial chemotaxis signaling pathway and their interactions. The diagram shows a core signaling complex with all the functional proteins described in text. The green spheres represent the four modification sites on each of the receptor monomers.

Chemoreceptors

E. coli has four transmembrane chemoreceptors (Hazelbauer et al., 2008; Hazelbauer & Lai, 2010), Tsr (taxis to serine and repellents), Tar (taxis to aspartate and repellents), Tap (taxis to dipeptides), Trg (taxis to ribose and galactose) that are also known as methyl-accepting chemotaxis proteins (MCPs) and another MCP-like protein, Aer (taxis to oxygen) that is anchored to membrane in the cytoplasm. Each of the MCPs has a periplasmic ligand-binding site and a conserved cytoplasmic signaling domain. They exist as homodimers and the cytoplasmic domains of two protomers form a four-helix coiled-coil structure as is shown in the crystal structure (Kim et al., 1999). The structure of the periplasmic domain has also been solved separately. With each protomer's four-helix bundle, the periplasmic ligand binding domain has a structure of eight helices (Milburn et al., 1991; Yeh et al., 1996). Fig. 6 shows a model of the structure of intact dimeric transmembrane receptor Tar. Each protomer has four methyl-accepting glutamyl residues in the cytoplasmic domain that can be methylated by methyltransferase CheR to form neutral glutamyl methylesters, a modification that results in a chemoreceptor conformational change that increases its ability to activate kinase (Springer & Koshland, 1977). These methylesters can be demethylated by methylesterase CheB to reform the negatively charged side chain, a modification that reduces kinase activity (Kehry & Dahlquist, 1982; Kehry et al., 1985). Receptors interact with CheW (Vu et al., 2012; Li et al., 2013; Pedetta et al., 2014) and CheA (Wang et al., 2012; Li et al., 2013; Piasta et al., 2013) at their cytoplasmic tip region (Figs. 3 & 4), the sequence of which is highly conserved not only within these four MCPs, but also among the chemoreceptor genes in

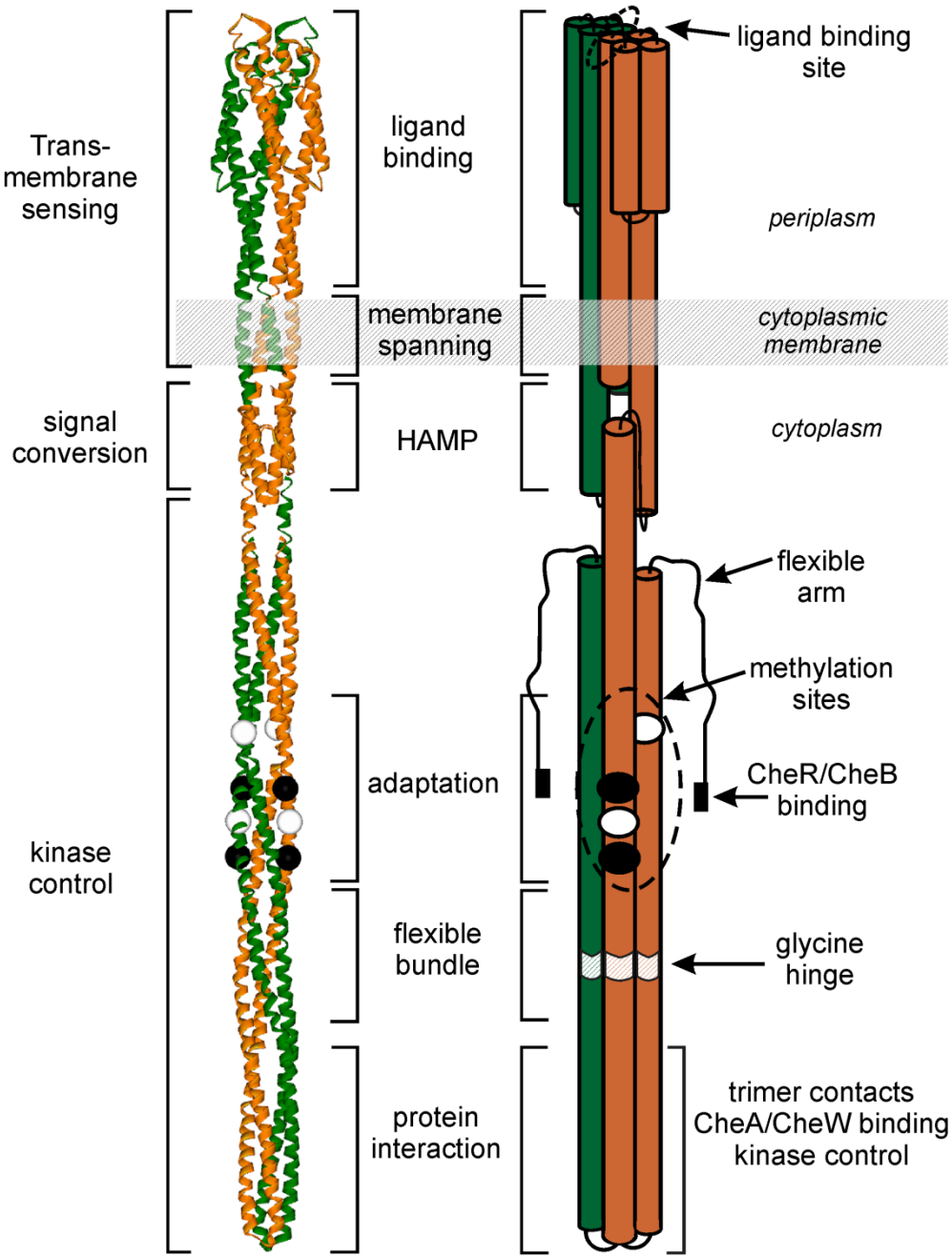

Fig. 6. Model of intact dimeric transmembrane receptor Tar, adapted from (Hazelbauer & Lai, 2010). The ribbon diagram is shown on the left. On the right is a cylinder diagram. Green and orange each represents one protomer. Each domain and other critical regions are labeled properly.

other species (Morgan et al., 1993; Zhulin, 2001). The sequences of the periplasmic sensing domains vary significantly, reflecting their different tasks as sensors. Tar, the receptor sensing amino acid aspartate, is the only receptor that has been used in this work.

CheA

In contrast to many class I histidine kinases like EnvZ (osmolarity sensor protein), and PhoQ (Mg^{2+} sensor) which are at the same time dimerized transmembrane receptors, chemotactic kinase CheA is a class II histidine kinase (Dutta et al., 1999) that is in the cytoplasm. It is active as a homodimer (Fig. 7) (Surette et al., 1996). Each protomer has five domains, P1 to P5 (Bilwes et al., 1999). Crystal structures of P1 (Mourey et al., 2001), P2 (McEvoy et al., 1998) and a dimer of P3-P4-P5 (Bilwes et al., 1999) have been solved separately.

P1 (PDB: 1I5N) has an up-down up-down four-helix bundle structure, typical for histidine phosphotransfer domains, and an additional C-terminal helix (Mourey et al., 2001). His48, the phospho-receiver is localized on the B helix and exposed to solvent. P2 binds response regulators CheY and CheB (SwansonBourret et al., 1993; Li et al., 1995), which facilitates the phosphoryl-transfer from P1 to those two substrates. However, without P2, CheA is still able to autophosphorylate and respond to receptor control and transfer the phosphoryl group on P1 to CheY and CheB at a reduced rate (Jahreis et al., 2004). P3 is the dimerization domain; two helices from each CheA protomer combine to form an inter-subunit four-helix bundle (Bilwes et al., 1999), which very much resembles the four-helix bundle core made with two transmembrane class I histidine kinase. P4 contains the kinase active site which is defined by conserved motifs N, G1, F and G2

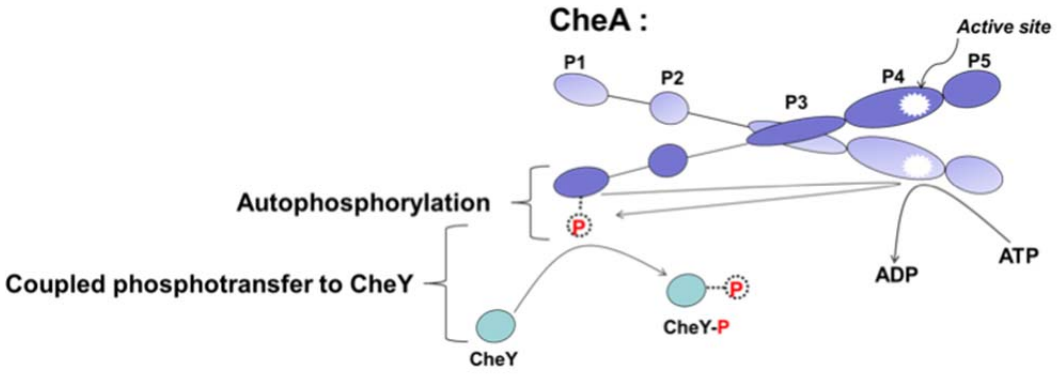

Fig. 7. Cartoon showing the trans-autophosphorylation of CheA and the coupled phosphotransfer to CheY. CheA is shown as a dimer with one promoter being purple and the other light purple. The ovals represent different domains. Solid lines between P1 and P2, P2 and P3 depict disordered linkers that give P1 and P2 domains great mobility. CheY is shown as cyan ovals.

boxes mentioned above (Parkinson & Kofoid, 1992; Stock et al., 2000) and thus binds both substrates, P1 and ATP. Regulatory domain P5 interacts with chemoreceptors and CheW to form core signaling complexes in which kinase activity is coupled to receptors and placed under their regulatory control (Li & Hazelbauer, 2011a; Briegel et al., 2012; Liu et al., 2012). Unstructured linkers of 25 residues between P1 and P2, and 32 residues between P2 and P3 (Levit et al., 1996; McEvoy & Dahlquist, 1997; McEvoy et al., 1997) provide considerable mobility for the self-contained P1 and P2 domains. According to the EM tomography by Briegel et al., this mobility of P1 and P2 is related to the signaling state of receptors when CheA is in signaling complexes, where they are more mobile with kinase-on receptors than with kinase-off receptors (Briegel et al., 2013). The NMR data from Hamel et al. indicate an alternative binding site for P1 on P4, away from the active site (Hamel et al., 2006). This unproductive binding could potentially happen for the less mobile, less active CheA.

CheW

As a small protein (167 residues, 18 kDa), CheW has a big role in bacterial chemotaxis. Although it doesn't possess any catalytic activity, CheW is essential for the formation of receptor-CheW-CheA complex (Fig. 5). The primary structure of CheW is highly conserved among different species (Wadhams & Armitage, 2004). The solution structure of CheW from hyperthermophile *Thermotoga maritima* (Griswold et al., 2002) revealed that it was similar to the regulatory domain P5 of CheA, sharing the SH3-like overall folding (PDB: 1K0S for *T. maritima* , 2HO9 for *E. coli*). Dahlquist lab (Gegner & Dahlquist, 1991) had showed that CheW and CheA form a complex, with the Kd being

17 μM. Without receptors, CheW can activate CheA modestly (McNally & Matsumura, 1991).

CheY

Structures of CheY (PDB: 2CHY) (Stock et al., 1989) and CheY in interaction with CheA P2 domain (PDB: 1A0O) (Welch et al., 1998) have been determined by NMR and X-ray crystallography. This compact globular protein (Fig. 5) has 128 residues (Stock et al., 1989) and is phosphorylated on the conserved Asp57 residue (Sanders et al., 1989). Once CheY is phosphorylated, the affinity between CheA and CheY is reduced (Li et al., 1995). At the same time, the affinity between CheY to the protein FliM of the flagellar motor is elevated, thus promoting clockwise flagellar rotation (Welch et al., 1993; Toker & Macnab, 1997; McEvoy et al., 1999).

CheR

The 274-residue methyltransferase CheR (Fig. 5) (PDB: 1AF7) plays an important role in the adaptation mechanism of bacterial chemotaxis (Djordjevic & Stock, 1998). Upon attractant binding, the receptors change their conformation and become better substrates for CheR that catalyzes the transfer of methyl groups donated by S-adenosylmethionine to four glutamate residues on each receptor (Springer & Koshland, 1977). These modifications change the conformation of receptors, making them suitable for kinase activation (Li & Weis, 2000). Thus the fully modified receptors activate kinase the most (Liberman et al., 2004).

CheB

The methylesterase CheB (Fig. 5) is the other response regulator that is activated upon phosphorylation by CheA. The 349-residue protein (PDB: 1A2O) has two distinct domains, an N-terminal regulatory domain and a C-terminal catalytic domain (Djordjevic et al., 1998). When the N-terminal Asp-56 is not phosphorylated, the regulatory domain blocks the active site of the catalytic domain. A conformational change is induced by phosphorylation at the regulatory domain (Anand et al., 1998; Anand & Stock, 2002), which allows access to the active site of the catalytic domain. Active CheB removes the methyl groups added by CheR to the four glutamate residues on each of the receptors, changing the conformation of the receptors to one that doesn't activate kinase CheA (Borkovich et al., 1992).

CheZ

CheZ (PDB: 1KMI) (Fig. 5) is composed of 214 residues, most (64%) of which are in helical structure (Zhao et al., 2002). This phosphatase plays an important role in the adaptation mechanism of the chemotaxis signaling system, bringing CheY-P back to unphosphorylated form for the next round of signaling. The co-crystal structure of CheY and CheZ indicates that a residue of CheZ may position a water molecule inline to attack the phosphoryl group on CheY-P (Zhao et al., 2002). Although CheY possesses intrinsic autodephosphorylation activity (Hess et al., 1987; Hess et al., 1988), the reaction of dephosphorylation of CheY-P is too slow for the response time of chemotaxis signaling system (Block et al., 1982). Fortunately, the interaction between CheZ and CheY-P decreases the half-life of CheY-P from ~20 seconds to ~200 milliseconds (Hess et al.,

1988; Wadhams & Armitage, 2004). This mechanism allows bacteria to respond to their environment in a very short period of time.

Kinetics of CheA

The analysis of autophosphorylation of CheA indicates this is a slow reaction, with a catalytic constant being approximately 0.026 s^{-1} (Tawa & Stewart, 1994). Another kinetic study of CheA and its catalytic fragment P3P4P5 reported higher values: 0.24 s^{-1} for CheA and 0.48 s^{-1} for P3P4P5 (Levit et al., 1999). The origins of these disparities could reflect several significant differences between the experimental designs of the two studies. Neither of these studies included intact chemoreceptors and investigation of the effects of ligand binding and receptor modifications. Thus we were interested in studying the kinetics of CheA to a greater extent and exploring the activities of CheA alone and in signaling complexes and the effects of ligand binding and receptor modifications on the activity of the kinase. This leads to our work described in Chapter Two.

CHAPTER TWO

Steady-state kinetic study of CheA P3-P4-P5

Note:

This chapter is based on our publication in Protein Science:

"Signaling complexes control the chemotaxis kinase by altering its apparent rate constant of autophosphorylation". (Pan et al., 2017)

which is featured as a highlighted paper in that issue.

Introduction

Outstanding question

Histidine kinase CheA (Fig. 8A) plays a central role in the signaling system of bacterial chemotaxis. Its activity determines cellular levels of the phosphorylated, i.e. active forms of response regulator CheY and the methylesterase of sensory adaptation, CheB. Control of kinase activity by transmembrane, methyl-accepting chemoreceptor proteins directs bacterial movement in favorable directions. CheA alone has very low kinase activity. As illustrated by the CheY-coupled phosphorelay, incorporation into signaling complexes with chemoreceptors and the coupling protein CheW activates CheA up to 1000-fold (Fig. 9) and places the enhanced activity under control of chemoreceptors (Borkovich et al., 1989; Ninfa et al., 1991; Li & Hazelbauer, 2011a). When attractants bind to the receptors in the signaling complexes, that enhanced kinase activity is inhibited. At saturation this inhibition is 50-fold to 100-fold (Fig. 9). Four methyl-accepting glutamyl residues in the receptor cytoplasmic domain can be methylated by methyltransferase CheR to form neutral glutamyl methylesters, a modification that results in a chemoreceptor conformational change that generates kinase activation. These methylesters can be demethylated by methylesterase CheB to reform the negatively charged side chain, a modification that reduces kinase activity. Glutaminyl residues at methyl-accepting sites have essentially the same effects as methylesters (Park et al., 1990; Dunten & Koshland, 1991) and thus manipulating a chemoreceptor gene to code for glutamines at those sites allows creation of receptors with defined extents and positions of adaptational modification. Kinase activation by a fully modified, all-glutamine receptor as measured by coupled phosphorylation of CheY is almost 200-fold

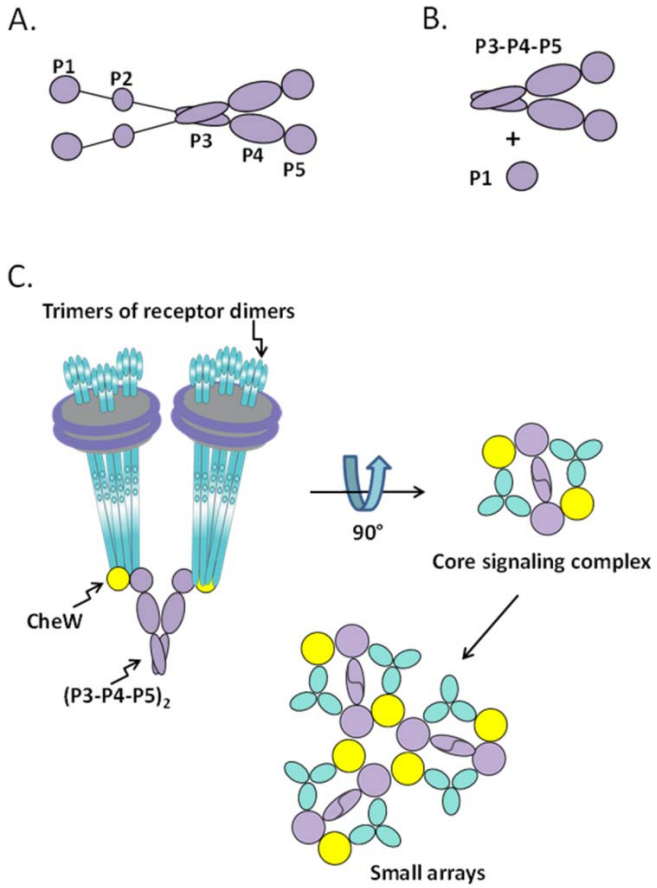

Fig. 8. Cartoon representations of autophosphorylating kinase CheA and chemotaxis signaling complexes. A. CheA homodimer. The five domains are shown as purple balls and ovals, labeled P1 through P5 for one protomer (see text). Lines between P1 and P2, and between P2 and P3 represent flexible linkers that provide mobility for P1 and P2. **B.** Liberated P1 and catalytic fragment P3-P4-P5. **C.** Signaling complexes of receptor-CheW-CheA P3-P4-P5. The left-hand cartoon represents a core signaling complex of two trimers of receptor dimers inserted into water-soluble Nanodiscs, two copies of coupling protein CheW and a CheA P3-P4-P5 dimer. The right-hand diagram is the view of the complex from its cytoplasmic tip. Core complexes can interact and expand to higher order array structures (bottom).

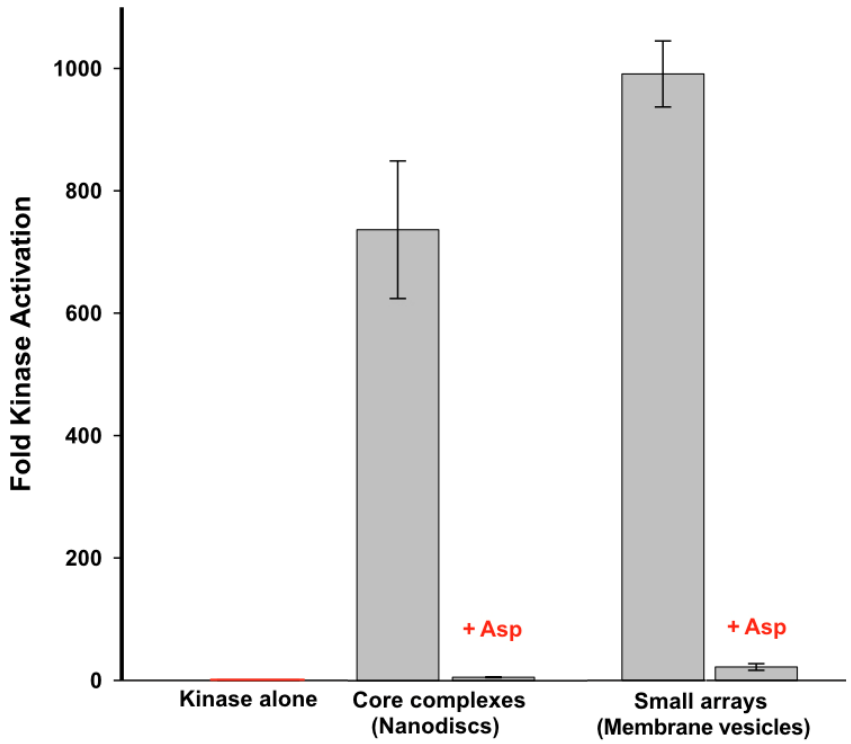

Fig. 9. CheY coupled reaction. Adapted from Li and Hazelbauer's (Li & Hazelbauer, 2011a). This histogram shows the kinase activity normalized to kinase alone. As kinase is incorporated into core complexes and small arrays of complexes, its activity is increased ~700-fold and ~1000 fold, respectively. When saturating ligand (Asp) concentration is applied, those activities decrease 100-fold and 50-fold, respectively.

greater than by an all-glutamate receptor (Amin & Hazelbauer, 2010b).

CheA is an autophosphorylating histidine kinase (Fig. 8). It forms homodimers (Gegner & Dahlquist, 1991). Only the dimeric form is enzymatically active (Surette et al., 1996). Each protomer has five domains (Fig. 8A) (Bilwes et al., 1999), namely P1 to P5. P1 carries the auto-phosphorylated histidine, His48. P2 binds CheY and CheB, bringing those substrate proteins in proximity to phosphorylated P1 and thus accelerating phosphoryl transfer. P3 is the dimerization domain. P4 contains the kinase active site and thus binds both substrates, P1 and ATP. Regulatory domain P5 interacts with chemoreceptors and CheW to form core signaling complexes in which kinase activity is coupled to receptors and placed under their regulatory control. An unstructured linker between P1 and P2, and another between P2 and P3, totaling ~60 residues of unstructured polypeptide chain, provide considerable mobility for the self-contained P1 and P2 domains (Levit et al., 1996; McEvoy & Dahlquist, 1997; McEvoy et al., 1997). Thus interaction of the P1 phosphoryl-accepting domain and the P4 active site occurs by diffusion of P1 on a relatively long tether. In fact, the "liberated", untethered form of P1 is phosphorylated by the P3-P4-P5 portion of the kinase (SwansonSchuster et al., 1993; Garzon & Parkinson, 1996; Levit et al., 1999). We have utilized this phenomenon in the experimental design of the current study.

Kinase activation upon formation of signaling complexes, kinase inhibition by chemoreceptor ligand occupancy and control of kinase activity by chemoreceptor adaptational modification must all alter crucial features of the enzymatic reaction. However, information about the identity of these features is limited and incomplete. Thus we performed Michaelis-Menten analysis of steady-state kinetics for kinase

autophosphorylation by CheA alone, CheA in core signaling complexes and CheA in small arrays of signaling complexes. For the latter two conditions, we determined autophosphorylation kinetics as a function of chemoreceptor ligand occupancy and adaptational modification.

Experimental strategy

The initial step in phosphoryl transfer by the chemotaxis two-component signaling system is autophosphorylation of kinase CheA. Our studies of kinase activation and inhibition characterized this reaction by steady-state, Michaelis-Menten analysis. There are two substrates in the autophosphorylation reaction, the phosphoryl-donor ATP and the phosphoryl-accepting histidine on the P1 domain of the kinase. One substrate, P1, is tethered to the active site. This situation limits and complicates steady-state kinetic characterization of autophosphorylation by intact kinase because the concentration of that substrate cannot be varied, the enzyme undergoes a single turnover and the phosphoryl group on P1 is readily transferred back to ADP (Greenswag et al., 2015). To overcome these limitations, we used P1 liberated by genetic manipulations from the enzymatically active module, domains P3-P4-P5 (Fig. 8B) (Garzon & Parkinson, 1996). Other investigators have shown that liberated P1 is effectively phosphorylated by domains P3-P4-P5 and the separated domains allow kinetic characterization of autophosphorylation (SwansonSchuster et al., 1993; Garzon & Parkinson, 1996; Levit et al., 1999).

A second design issue was the possibility of local trapping of ATP or liberated P1 near the active site. Specifically, in arrays of signaling complexes, there are multiple kinase active sites in close proximity. Since substrates generally interact with active sites many times before catalysis occurs (Williamson, 2012), high local concentrations of substrate-

binding sites could retain substrates near the active site, generating effective local concentrations higher than bulk concentrations and thus confounding kinetic analysis based on values of bulk concentrations. We addressed this issue by characterizing kinase autophosphorylation in isolated signaling complexes assembled using Nanodisc- inserted chemoreceptors (Boldog et al., 2006; Li & Hazelbauer, 2014) and compared those results to kinase autophosphorylation by the small arrays of signaling complexes that assemble on chemoreceptors inserted in native membranes fragments isolated from cells overproducing those receptors (Fig. 8C) (Briegel et al., 2014).

Results

Kinetic analysis of CheA autophosphorylation

We performed steady-state kinetic analysis of P1 phosphorylation by CheA P3-P4-P5 alone (Fig. 10) and incorporated into individual, Nanodisc-based core signaling complexes assembled using the *Escherichia coli* aspartate receptor Tar in its native gene-encoded, intermediate modification state of the four methyl-accepting sites: glutamine, glutamate, glutamine, glutamate (QEQE), at sites 1 through 4, respectively (Fig. 11). Initial rates of P1 phosphorylation by P3-P4-P5 (Fig. 12), which are equivalent to initial rates of autophosphorylation for intact CheA, were determined as a function of variable concentrations of one substrate or the other (ATP or P1) in the presence of a constant concentration of the second substrate (P1 or ATP). For signaling complexes, these studies were repeated in the presence of aspartate, a Tar-recognized chemoattractant. The effects of this receptor ligand were examined at two concentrations: 5 μM, almost two-fold above the half-maximal inhibitory concentration of 2.8 μM (Fig. 13), and 20 μM, equivalent to 88% receptor saturation (Figs. 11 and 13). As observed in previous studies (Borkovich et al., 1989; Borkovich & Simon, 1990; Li & Hazelbauer, 2011a), incorporation of kinase into signaling complexes greatly enhanced phosphorylation and the presence of an attractant ligand significantly reduced it.

From these primary data we determined for each substrate kinetic parameters of P1 phosphorylation: the apparent catalytic constant k_{cat}, the Michaelis constant K_M and the catalytic efficiency k_{cat}/K_M (Tables I and II). K_M values were determined directly from data plots by fitting to a modified Michaelis-Menten equation. Values for k_{cat} were calculated from the respective data sets, one generated by varying ATP concentration and

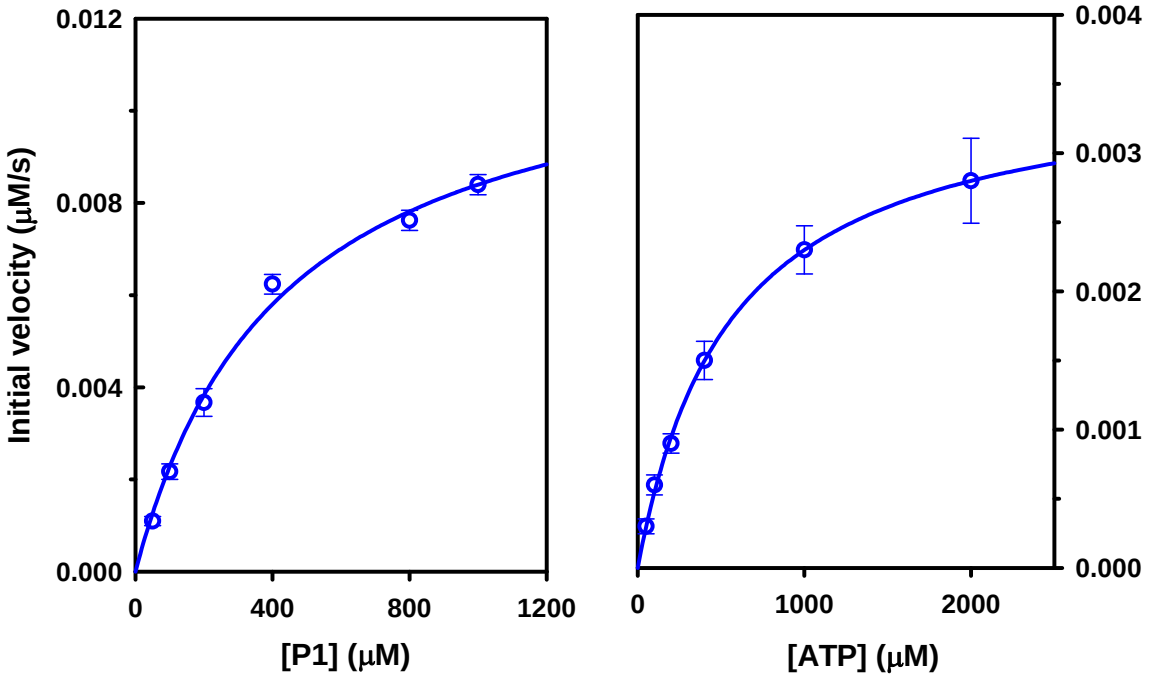

Fig. 10. P1 phosphorylation by CheA P3-P4-P5 alone. The data are the same as shown in Fig. 11, but with an expanded y-axis to facilitate illustration of the pattern of initial velocity as a function of substrate concentration.

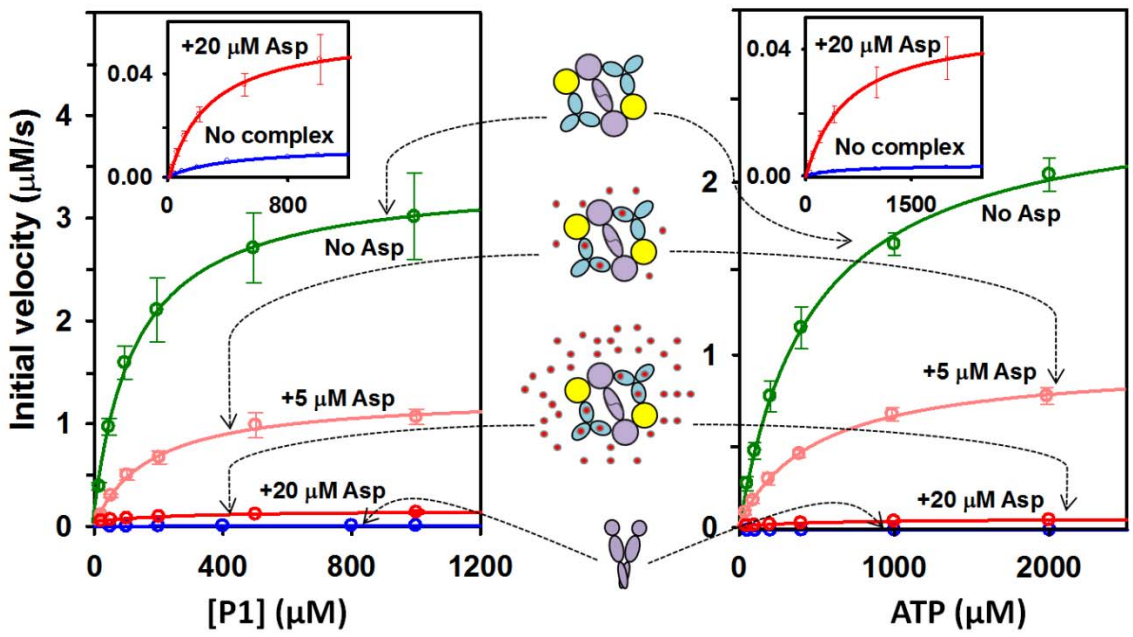

Fig. 11. P1 phosphorylation by CheA P3-P4-P5. Mean values of initial rates as a function of concentration of P1 (left) or ATP (right) in the presence of a constant concentration of the other substrate (1000 μM ATP or 100 μM P1, respectively) are shown for P3-P4-P5 alone (blue) and in core complexes with Tar in the absence of ligand (green), plus 5 μM (pink) or 20 μM aspartate (red). Cartoons between the two panels illustrate the various conditions. Red dots represent Asp. The inset shows an expanded scale for two lowest curves. Fig. 10 provides a further expansion for the lowest curve, P3-P4-P5 alone. To facilitate direct comparisons, initial rates were normalized to 1.8 μM P3-P4-P5. Error bars represent standard deviations of the mean ($n \geq 3$).

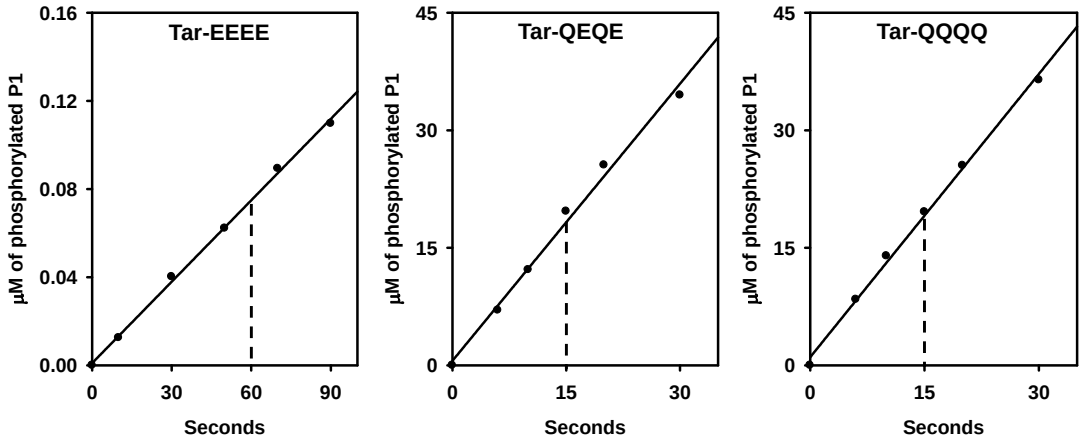

Fig. 12. Representative timecourses of phosphorylation of liberated P1 by CheA P3-P4-P5. Small arrays of signaling complexes were assembled using individual native membrane preparations, each containing chemoreceptor Tar with a different state of adaptational modification. Each kind of signaling complex was mixed with 220 µM P1 and 1000 ATP, and phosphorylated P1 determined at the times indicated. A. Tar-EEEE in complexes providing 0.36 µM P3-P4-P5. B. Tar-QEQE in complexes providing 0.45 µM P3-P4-P5. C. Tar-QQQQ in complexes providing 0.52 µM P3-P4-P5. Such time courses were used to identify sampling times used to measure initial rates of P1 phosphorylation. For each plot, dashed lines mark the sampling time chosen for each receptor modification state.

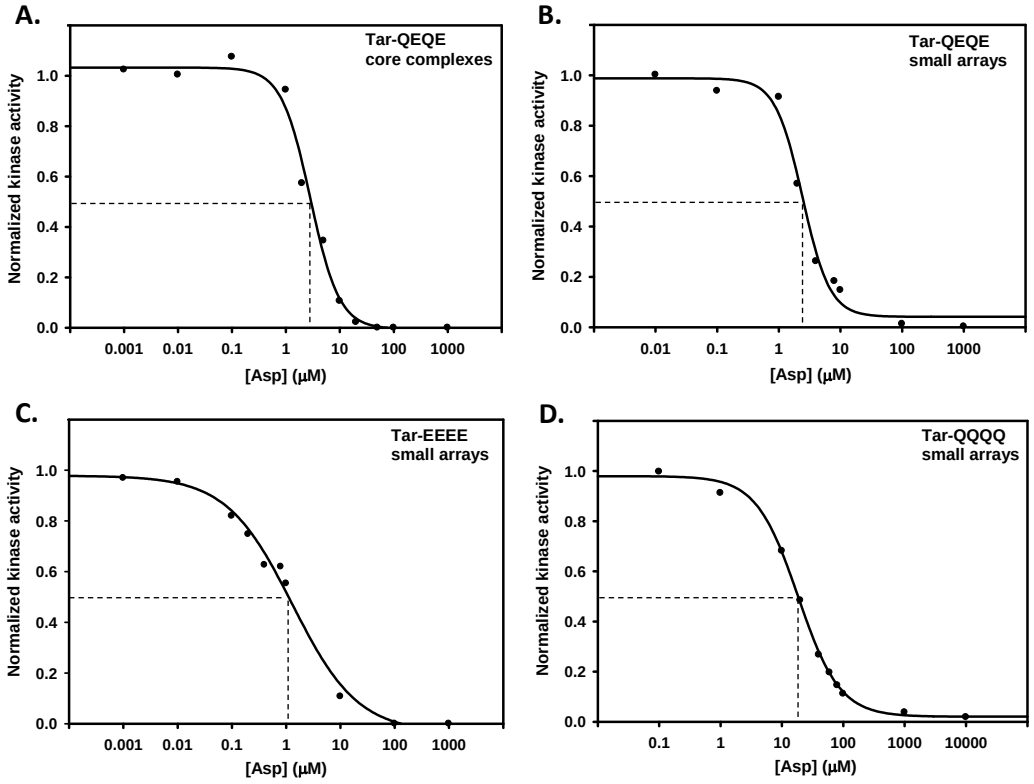

Fig. 13. Inhibition of kinase activity as a function of aspartate concentration. CheA P3-P4-P5 incorporated into signaling complexes with chemoreceptor Tar were assayed for phosphorylation of liberated P1 in the presence of 220 μM P1, 1000 μM ATP and the indicated concentrations of the Tar attractant ligand aspartate. Initial velocities at each concentration were normalized to the initial velocity in the absence of aspartate and plotted as a function of aspartate concentration. Dashed lines mark the $[Asp]_{½}$, the ligand concentration at which kinase is inhibited 50%. A. Nanodisc-based core complexes assembled with Tar-QEQE, $[Asp]_{½}$ = 2.8 μM. Native-membrane-based small arrays of core complexes assembled with: B. Tar-QEQE, $[Asp]_{½}$ = 2.4 μM . C. Tar-EEEE, $[Asp]_{½}$ = 1.3 μM D. Tar-QQQQ, $[Asp]_{½}$ = 18 μM.

the other by varying P1 concentration. We divided the V_{max} determined using Michaelis-Menten fitting of the primary data by the concentration of enzyme, i.e. P3-P4- P5. For P3-P4-P5 alone the enzyme concentration was the concentration of P3-P4-P5 in the reaction mixture. For kinase in Nanodisc-based, single core complexes, the relevant enzyme concentration was the concentration of P3-P4-P5 incorporated into signaling complexes. We determined that concentration by utilizing the receptor-borne affinity tag to separate P3-P4-P5 incorporated into Nanodisc-based core complexes from unassociated enzyme (see Materials and Methods). The two resulting apparent k_{cat} values were adjusted using the K_M value of the respective substrate that had been held constant at a sub-saturating concentration to determine the catalytic constant of catalysis at saturation of both substrates (see Materials and Methods). Thus we obtained two separate determinations of the overall catalytic constant of P1 phosphorylation. The resulting values were the same within the error of the determinations (Tables I and II). This provided an important internal check of the validity of our measurements and calculations. For each condition, the separate values were averaged to yield a best estimate of the apparent catalytic constant of CheA autophosphorylation. That averaged value was used to calculate values for k_{cat}/ K_M, a measure of enzymatic catalytic efficiency.

Fig. 14 illustrates that kinase activation in signaling complexes affected primarily kcat, enhancing that parameter 300-fold, modestly improved K_M^{P1} i.e. decreased its value (3.3-fold) and did not significantly change K_M^{ATP}. These changes enhanced k_{cat}/K_M^{ATP} 350-fold and k_{cat}/K_M^{P1} 1000-fold. Similarly, as illustrated in Fig. 15, aspartate at 88% receptor saturation reduced k_{cat} almost 40-fold, increased K_M^{P1} 2.1-fold and had no significant

effect on K_M^{ATP}, resulting in respective k_{cat}/K_M values reduced to 1.3% and 2.2% of the ligand-free condition.

Comparison of isolated core complexes and small arrays

We compared activation and ligand control of CheA P3-P4-P5 in Nanodisc-based, isolated core signaling complexes (Fig. 11 and Table I) to activation and control in small arrays of core complexes (Fig. 16) assembled using *E. coli* membrane isolated from cells overproducing a chemoreceptor (Fig. 17 and Table II). Comparable small arrays, assembled with intact kinase, have been used extensively by multiple laboratories to characterize in vitro receptor-controlled signaling (Borkovich et al., 1992; Morrison & Parkinson, 1997; Li & Weis, 2000; Bornhorst & Falke, 2001; Lai et al., 2005; Erbse & Falke, 2009; Amin & Hazelbauer, 2010b). To determine k_{cat} values for signaling complexes formed on Tar-containing native membrane vesicles, we determined the amount of CheA P3-P4-P5 incorporated into those complexes by quantifying P3-P4-P5 retained by the membranes after centrifugation and washing to remove free enzyme (Erbse & Falke, 2009). As illustrated in Fig. 17, there were no systematic differences between the two preparations in terms of signaling complex-mediated activation or ligand-mediated inhibition of kinase autophosphorylation. Thus, it appears that small arrays of core complexes do not significantly confound kinetic analysis because of increased local substrate concentrations generated by the presence of multiple closely clustered substrate-binding sites. On the basis of this information, we used the small arrays of signaling complexes assembled on native membranes containing inserted Tar to investigate effects of adaptational modification.

Table I. Kinetic constants for P1 phosphorylation by P3-P4-P5 alone and in core complexes assembled with Tar-QEQE ± Asp

Kinase	[Asp] (μM)	Vary [P1]		Vary [ATP]		Mean k_{cat}[a] (s^{-1})	k_{cat}[a]/K_M^{P1} (10^3 M^{-1} s^{-1})	k_{cat}[a]/K_M^{ATP} (10^3 M^{-1} s^{-1})
		K_M (μM)	k_{cat} (s^{-1})	K_M (μM)	k_{cat} (s^{-1})			
Alone	0	430 ± 61	0.010 ± 0.001	550 ± 37	0.010 ± 0.001	0.010 ± 0.001	0.023 ± 0.004	0.018 ± 0.002
Core compl.	0	130 ± 20	2.8 ± 0.5	480 ± 93	3.2 ± 0.03	3.0 ± 0.2	23 ± 4	6.3 ± 1.3
Core compl.	5	180 ± 6	1.0 ± 0.1	520 ± 160	1.5 ± 0.2	1.3 ± 0.1	7.1 ± 0.7	2.4 ± 0.8
Core compl.	20	270 ± 80	0.068 ± 0.001	600 ± 89	0.10 ± 0.02	0.084 ± 0.012	0.31 ± 0.10	0.14 ± 0.03

[a] Average of the k_{cat} values in columns 4 and 6.

Table II. Kinetic constants for P1 phosphorylation by P3-P4-P5 in small arrays of core complexes with Tar-QEQE ± Asp

[Asp] (μM)	Vary [P1]		Vary [ATP]		Mean k_{cat}[a] (s^{-1})	k_{cat}[a]/K_M^{P1} (10^3 M^{-1} s^{-1})	k_{cat}[a]/K_M^{ATP} (10^3 M^{-1} s^{-1})
	K_M (μM)	k_{cat} (s^{-1})	K_M (μM)	k_{cat} (s^{-1})			
0	120 ± 17	2.2 ± 0.3	330 ± 6	2.4 ± 0.3	2.3 ± 0.2	19 ± 3	7.0 ± 0.7
5	100 ± 6	0.53 ± 0.13	390 ± 47	0.77 ± 0.15	0.65 ± 0.10	6.3 ± 1.0	1.7 ± 0.3
100	150 ± 70	0.13 ± 0.01	560 ± 78	0.20 ± 0.02	0.17 ± 0.01	1.1 ± 0.5	0.29 ± 0.05

[a] Average of the k_{cat} values in columns 3 and 5.

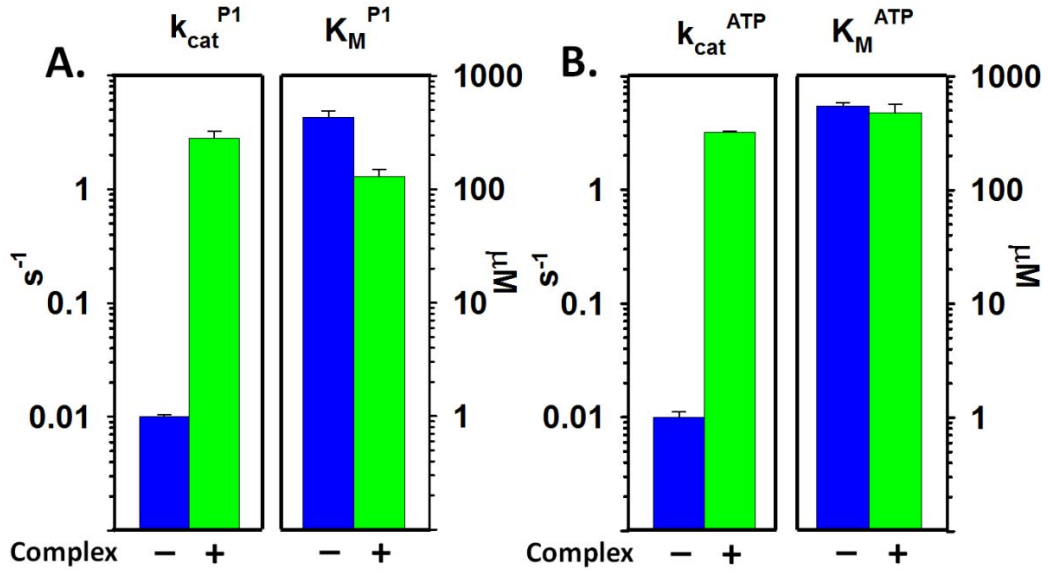

Fig. 14. Comparison of kinetic parameters derived from the data in Fig. 11 for P3-P4-P5 alone and in core signaling complexes. Mean values determined by varying P1 (A) or ATP (B) for k_{cat} (left-hand pairs of bars) and K_M (right-hand pairs of bars) are displayed on logarithmic scales. Error bars represent standard deviations of the mean ($n \geq 3$). See Table I for numerical values.

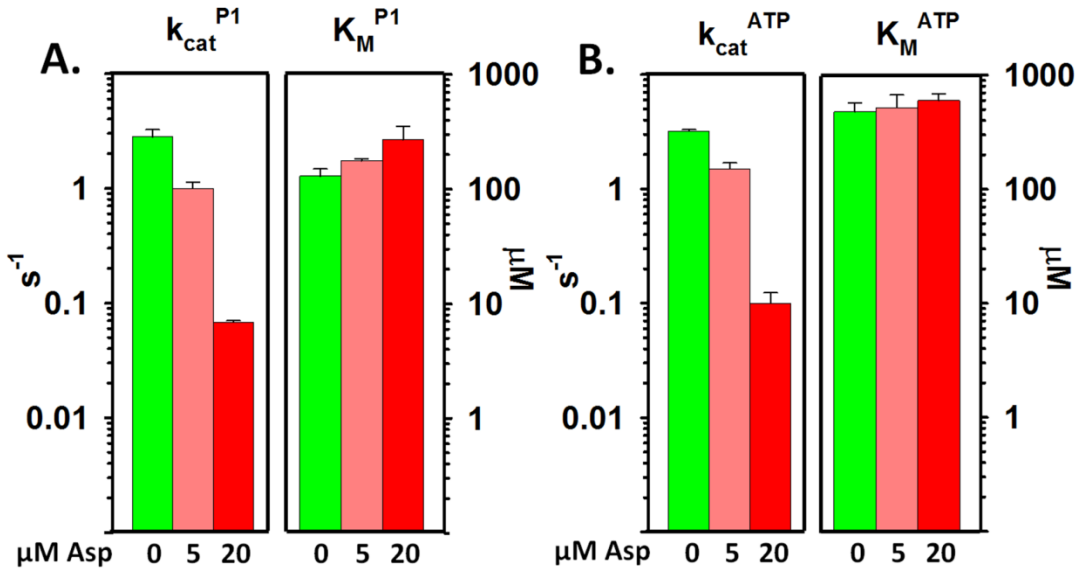

Fig. 15. Comparison of kinetic parameters for P3-P4-P5 in core complexes in the absence and presence of the Tar ligand aspartate. Mean values determined by varying P1 (A) or ATP (B) for k_{cat} (left-hand sets of bars) and K_M (right-hand sets of bars) in the absence (green) or presence of 5 μM (pink) or 20 μM (red) aspartate are displayed on logarithmic scales. Error bars represent standard deviations of the mean ($n \geq 3$). See Table I for numerical values.

Kinetic analysis of effects of chemoreceptor modification state on kinase autophosphorylation

It has long been observed that kinase activity of signaling complexes increases as chemoreceptor modification increases (Borkovich et al., 1992; Li & Weis, 2000; Bornhorst & Falke, 2001). We investigated the kinetic basis of these activity changes with analysis of P1 phosphorylation by P3-P4-P5 in small arrays of signaling complexes containing Tar at the two extremes of adaptational modification: none, glutamyl residues at the four methyl-accepting sites (Tar-EEEE); and complete, glutaminyl residues at the four sites (Tar-QQQQ). The kinetic parameters derived from these data are shown in Table III and plotted in Fig. 18, along with the previously considered parameters for signaling complexes assembled with intermediate- modification-state receptor Tar-QEQE (Figs. 11, 14, 15; Table III). Those parameters indicate that the increase in kinase activity from no receptor modification to complete modification reflected in large part enhancement of k_{cat}, ~160-fold, and modest reductions of K_M^{ATP} and K_M^{P1} values, 3.2-fold and 1.6-fold, respectively. These changes resulted in enhancements of k_{cat}/K_M values 250-fold for P1 and 500-fold for ATP. Addition of a near-saturating concentration of the Tar ligand aspartate to signaling complexes formed with Tar in the two extremes of adaptational modification followed the pattern observed for Tar in the intermediate modification state (Table II and III; Fig. 18). The principal change upon ligand occupancy was in k_{cat} with no changes outside the error bars for K_M^{P1} and modest changes in K_M^{ATP}. Those modest changes would account for only a small portion of the observed kinase inhibition by ligand occupancy.

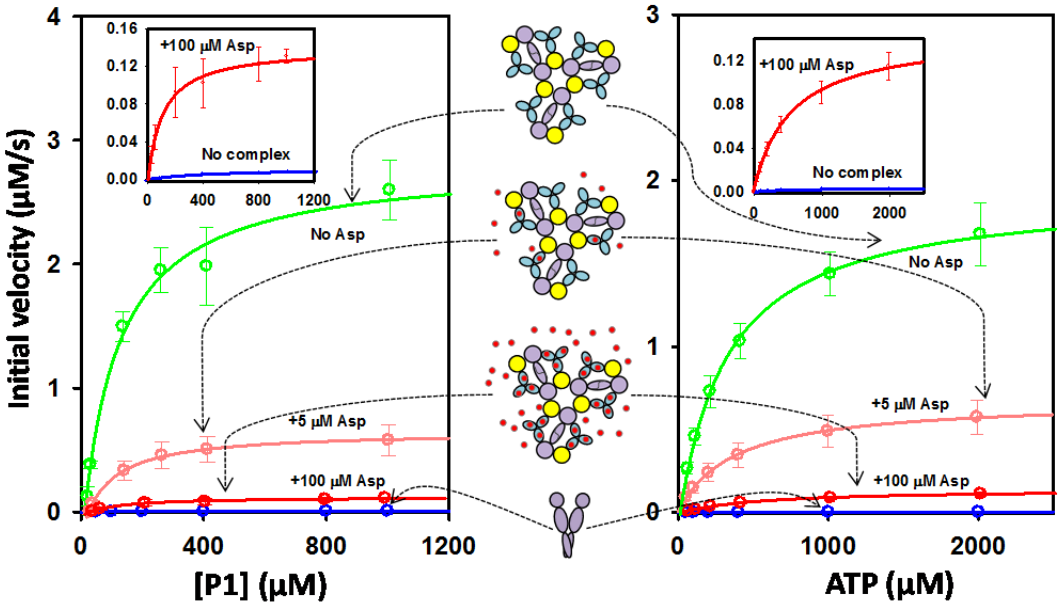

Fig. 16. P1 phosphorylation by CheA P3-P4-P5. Mean values of initial rates as a function of concentration of P1 (left) or ATP (right) in the presence of a constant concentration of the other substrate (1000 μM ATP or 100 μM P1, respectively) are shown for P3-P4-P5 alone (blue) and in small arrays of core complexes assembled with native-membrane-embedded Tar-QEQE in the absence of ligand (green), plus 5 μM (pink) or 100 μM aspartate (red). Cartoons between the two panels illustrate the various conditions. Red dots represent Asp. The inset shows an expanded scale for two lowest curves. To facilitate direct comparisons, initial rates were normalized to 1.8 μM P3-P4-P5, 100 μM P1 (when ATP is the variable substrate) or 1000 μM ATP (when P1 is the variable substrate). Error bars represent standard deviations of the mean ($n \geq 3$).

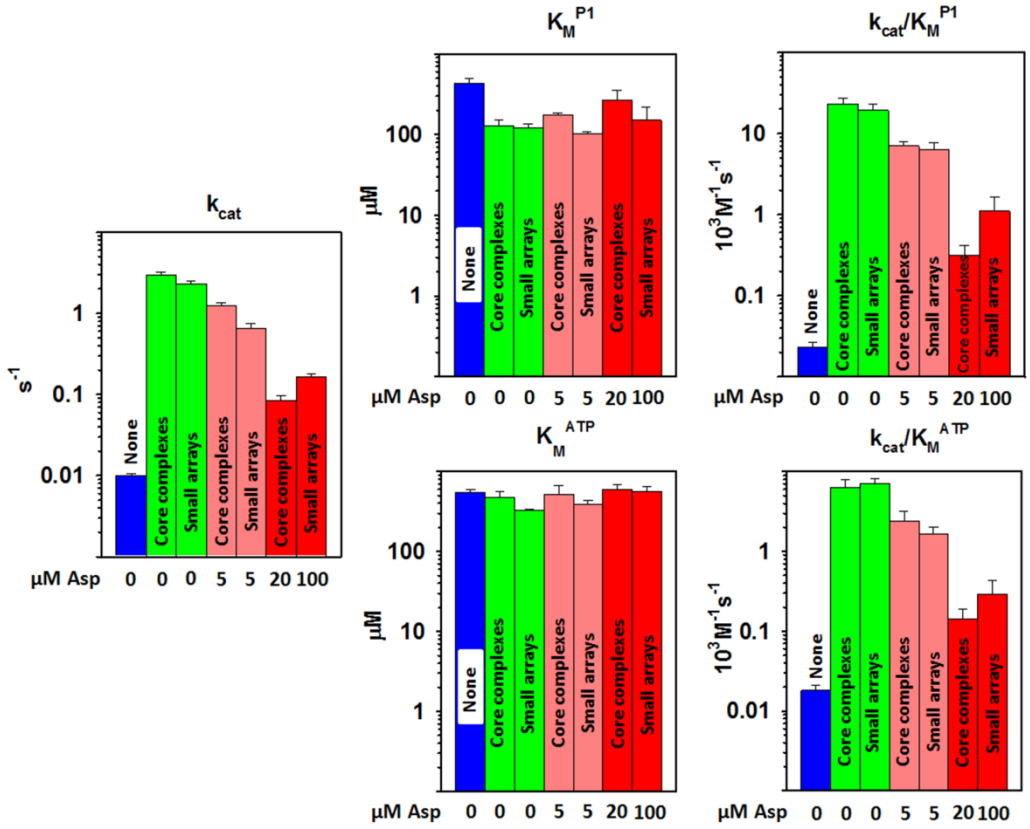

Fig. 17. Comparison of kinetic parameters for P3-P4-P5 alone, in core complexes and in small core complex arrays. Each set of bar graphs displays kinetic parameters on logarithmic scales for CheA P3-P4-P5 alone (blue), in core complexes or small arrays of those complexes with aspartate at 0 µM (green), 5 µM (pink) or a concentration close to saturating (20 or 100 µM; red). The left-hand plot shows the mean of k_{cat} values determined by varying P1 or ATP. The middle and right-hand plots show mean K_M and k_{cat}/K_M values for P1 (upper) and ATP (lower). Error bars represent standard deviations of the mean ($n \geq 3$). See Tables I and II for numerical values.

Table III. Kinetic constants for P1 phosphorylation by P3-P4-P5 in small arrays of core complexes as function of Tar modification and [Asp]

Tar modification	[Asp] (μM)	Vary [P1]		Vary [ATP]		Mean k_{cat}[a] (s^{-1})	k_{cat}[a]/K_M^{P1}	k_{cat}[a]/K_M^{ATP}
		K_M (μM)	k_{cat} (s^{-1})	K_M (μM)	k_{cat} (s^{-1})		(10^3 M^{-1} s^{-1})	(10^3 M^{-1} s^{-1})
EEEE	0	210 ± 26	0.027 ± 0.003	940 ± 280	0.033 ± 0.005	0.030 ± 0.003	0.14 ± 0.02	0.032 ± 0.010
EEEE	10	210 ± 29	0.0072 ± 0.0013	3100 ± 950	0.0066 ± 0.0011	0.0068 ± 0.0008	0.033 ± 0.006	0.0022 ± 0.0007
QEQE	0	120 ± 17	2.2 ± 0.3	330 ± 6	2.4 ± 0.3	2.3 ± 0.2	19 ± 3	7.0 ± 0.7
QEQE	100	150 ± 70	0.13 ± 0.01	560 ± 78	0.20 ± 0.02	0.17 ± 0.01	1.1 ± 0.5	0.29 ± 0.05
QQQQ	0	130 ± 21	5.2 ± 1.2	290 ± 15	4.1 ± 1.0	4.7 ± 0.8	35 ± 8	16 ± 3
QQQQ	1000	130 ± 15	0.18 ± 0.05	380 ± 120	0.19 ± 0.04	0.19 ± 0.03	1.5 ± 0.3	0.49 ± 0.18

[a] Average of the k_{cat} values in columns 4 and 6. QEQE data from Table II.

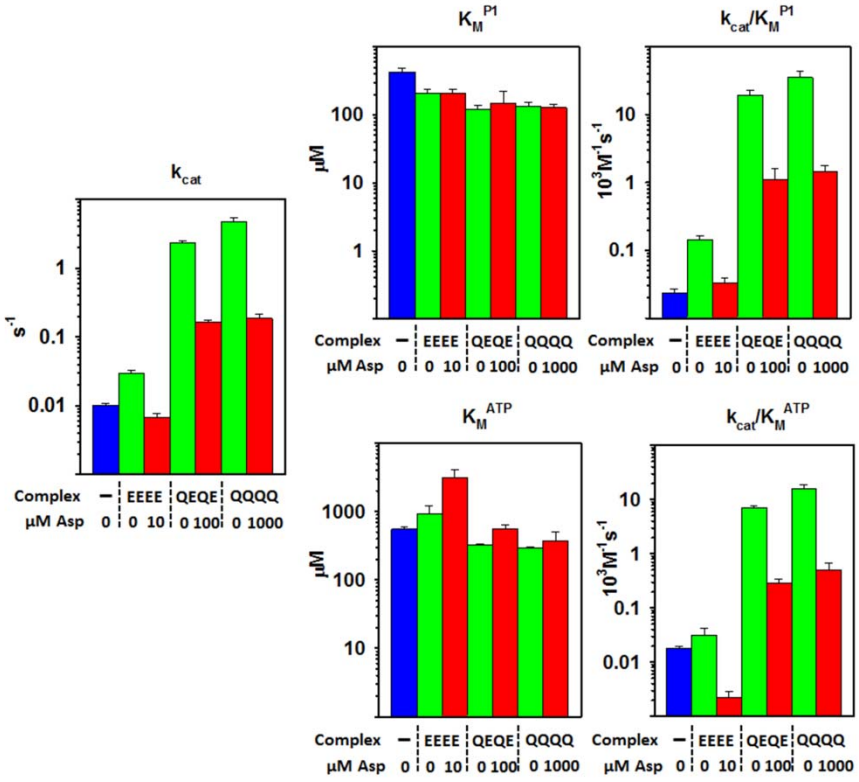

Fig. 18. CheA P3-P4-P5 kinetic parameters in small arrays of core complexes as a function of receptor modification state. Each set of bar graphs displays kinetic parameters on logarithmic scales for CheA P3-P4-P5 alone (blue), in small arrays of core complexes with chemoreceptor Tar at the indicated modification state and aspartate at 0 μM (green) or a concentration close (see Fig. 13) to saturating (red). The left-hand plot shows the averages of k_{cat} values determined by varying P1 or ATP. The middle and right-hand plots show mean K_M and k_{cat}/K_M values for P1 (upper) and ATP (lower). Error bars represent standard deviations of the mean ($n \geq 3$). See Table III for numerical values.

Discussion

Studies described here revealed that both activation and inhibition of CheA autophosphorylation are mediated primarily by changes in the apparent caalytic constant of phosphoryl transfer to the kinase P1 domain, that simple sequestration of the phosphoryl-accepting CheA domain P1 is not a major contributor to kinase control and that K_M values for P1 and ATP are poised near the estimated concentrations of the natively tethered domain and cellular ATP, respectively. In addition, as discussed in a following section, comparison of our data for P1 phosphorylation with data for coupled phosphorylation of response regulator CheY indicates that most of the control of kinase-mediated signaling is at the level of autophosphorylation, not at the level of phosphoryl transfer to the response regulator. We consider these observations in more detail in the sections below, after a brief discussion of the relationship of kinetic parameters we determined to parameters reported in previous studies.

Previous publications have reported values for a few of the kinetic parameters determined in the current study. Values we determined for those parameters are in large part consistent with published values. Our values for K_M^{ATP} (Tables I-III) are within the 170 to 770 μM range of published values for intact CheA, the CheA catalytic domain or either enzyme form in signaling complexes (Wylie et al., 1988; Borkovich et al., 1989; Tawa & Stewart, 1994; Alon et al., 1999; Levit et al., 1999). The 0.01 s^{-1} apparent catalytic constant (k_{cat}) we determined for phosphorylation of liberated P1 by isolated P3-P4-P5 was close to but lower than the 0.026 s^{-1} value determined by an extensive kinetic characterization of intact CheA autophosphorylation (Tawa & Stewart, 1994), perhaps because of a modest difference between catalytic constants for the liberated and tethered

domain. In contrast, a kinetic study of CheA and its catalytic fragment P3-P4-P5 as isolated enzymes and in signaling complexes assembled with receptor fragments reported quite different values for k_{cat}, ~10-fold higher for the intact enzyme and 48-fold higher for P3-P4-P5 (Levit et al., 1999). That study also reported K_M^{P1} values approximately 20-fold lower than the values we determined (Tables I-III). The origins of these disparities are not clear, but could reflect several significant differences between the experimental designs of the two studies. Importantly, the earlier study did not characterize intact signaling complexes but instead complexes of CheW, and CheA with chemoreceptor cytoplasmic domains lacking periplasmic and transmembrane domains and thus membrane association, and which exhibited with an apparent stoichiometry and three-dimensional organization different from those for the intact system (Francis et al., 2004). In addition, the earlier study was performed using *Salmonella enterica* chemotaxis proteins and an assay that monitored phosphorylation by coupled reactions monitoring steady-state phosphorylation not initial rate.

Kinase autophosphorylation is controlled via k_{cat}

Chemotaxis kinase CheA is influenced by three different inputs. It is activated by formation of chemotaxis signaling complexes, inhibited by ligand occupancy of receptors in those complexes and activated in complexes by covalent modifications that eliminate the negative charges of specific glutamyl residues at the receptor methyl- accepting sites. We investigated which features of enzyme activity were affected by the respective inputs and found that the major effect for all three was on the apparent catalytic constant of the reaction, k_{cat}. In some conditions the value of a substrate K_M was altered, but no more than approximately three-fold, not the orders of magnitude changes observed for the

apparent value of k_{cat}. In interpreting these observations, we can consider K_M values approximations of substrate dissociation constants because P1 phosphorylation by P3-P4-P5 fulfills the requirements of no known enzyme-substrate covalent intermediate and dissociation of enzyme-substrate complex much more likely than catalysis. The latter situation results from low apparent catalytic constants (<10 s^{-1}) and K_M values in the hundreds of micromolar. This indicates that the principal target of all three ways of affecting kinase activity is the catalytic constant of catalysis and not affinity of the enzyme for either substrate.

Thus we conclude that the effects we observed on the apparent values of k_{cat} are effects on the rate-limiting step of the catalytic mechanism. That step could be chemical transfer of the phosphoryl group from ATP to the histidinyl side chain of P1, release of product phospho-P1, release of ADP, or some other aspect of the catalytic cycle. Our data are consistent with complex formation, ligand binding and adaptational modification all targeting the same rate-limiting step for acceleration or deceleration. However, the situation could be more complex if the identity of the rate-limiting step changed upon activation or inhibition. In any case, k_{cat} could be changed in a pattern consistent with our data by action on the kinase active site to alter its effectiveness directly or by shifting an equilibrium between active and inactive conformations of that site (Greenswag et al., 2015).

Kinase control is almost entirely control of autophosphorylation

Chemotactic responses are the result of controlled changes in the cellular content of the phosphorylated form of response regulator CheY. Formation of CheY-P involves two

steps, phosphoryl transfer from ATP to a histidinyl residue on CheA domain P1 and phosphoryl transfer from P1 to response regulator CheY. Physiologically relevant kinase activity could be controlled at one or both steps. The work described here documents significant control of CheA autophosphorylation. Is there additional control at the step of phosphoryl transfer from P1-P to CheY? Comparisons of the data from this study with previous studies (Fig. 19) indicate that there could be modest additional control at that step, but that its magnitude would be small in relation to the overall change in kinase activity. Specifically, Nanodisc-based core complexes made with Tar-QEQE and assembled with CheA P3-P4-P5 increased the catalytic constant of kinase autophosphorylation ~350-fold and k_{cat}/K_M 350-to-1000-fold for P1 and ATP, respectively (Table I). Nanodisc-based Tar-QEQE core complexes assembled with intact CheA activated the rate of CheY-P formation ~750-fold. Comparison of these respective enhancements indicates that any contribution to activation of physiologically relevant kinase activity by phosphoryl transfer from P1-P to CheY would be no more than two-fold. Correspondingly, saturation with attractant ligand of chemoreceptors in core complexes made with CheA P3-P4-P5 inhibited the k_{cat} of autophosphorylation ~40-fold and k_{cat}/K_M in the order of 50-fold (Table I) whereas ligand saturation of intact CheA complexes inhibited the rate of CheY-P formation ~135-fold, implying no more than a three-fold contribution to inhibition of phosphoryl transfer from P1-P to CheY.

P1 sequestration at a site distinct from and unlinked to the active site is not a major contributor to kinase control

One means of controlling kinase activity of the intact enzyme would be to control availability of tethered P1, for instance by sequestering the domain at a binding site away

from the kinase active site. In fact, a P1-binding site separate from the active site has been identified on the CheA P4 domain (Hamel et al., 2006) and proposed on chemoreceptors (Morrison & Parkinson, 1997). In addition, tomographic images of signaling complex arrays revealed that in kinase-off signaling states the P1 and P2 domains of the intact kinase were sufficiently immobilized that they were visible as distinct densities in the sub-volume averages, but were not resolved in sub-volume averages of kinase-on signaling states (Briegel et al., 2013). These observations suggest that low kinase activity could correspond to immobilized, perhaps sequestered P1 domains. Our studies of kinase autophosphorylation using liberated P1 domains provided an opportunity to test the importance of sequestering P1-binding sites in control of kinase activity. In our experiments, liberated P1 was at concentrations of hundreds of micromolar whereas signaling complexes and their constituent proteins were at concentrations 100- to 1000-fold lower (Fig. 20). As a result, any P1-binding sites capable of sequestering the single P1 available to the active site of intact CheA would be occupied, but many P1 domains would still be available for interaction and catalysis at the kinase active site. If simple sequestering of tethered P1 were a major contributor to the kinase-off state, or release of sequestered P1 were a major contributor to its kinase-on state, then in experiments with liberated P1 and the catalytic P3-P4-P5 fragment, activity differences between the kinase-off and kinase-on states would have been significantly reduced or eliminated. Instead activation and inhibition of kinase corresponded, within a factor of two or three to the orders-of-magnitude effects observed for intact enzyme (Fig. 19). P1 sequestration at a site distinct from the active site could be involved in the remaining factor of two or three.

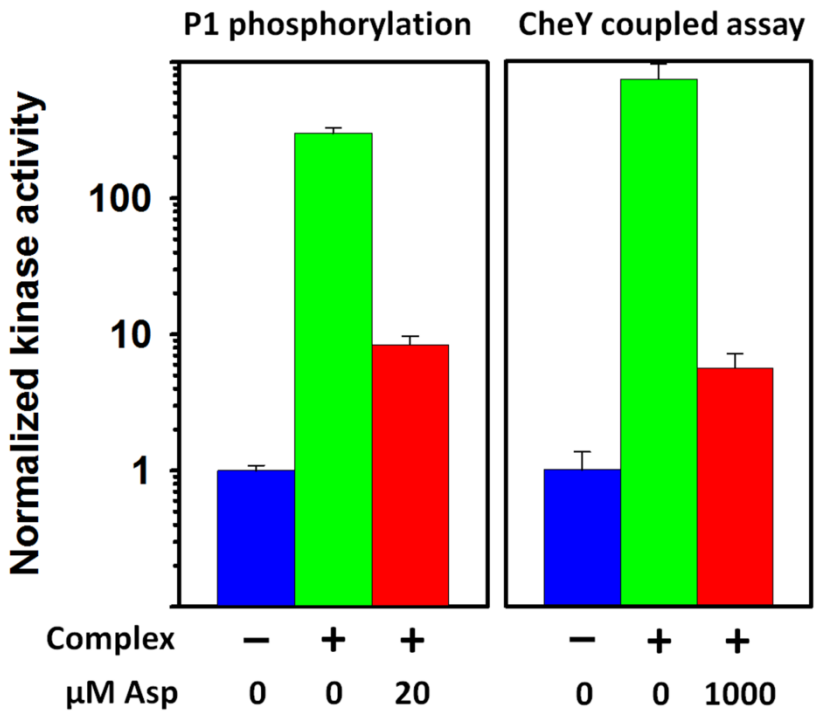

Fig. 19. Comparison of modulation of kinase autophosphorylation and modulation of coupled phosphorylation of CheY. Kinase activities normalized for each assay to the value for isolated kinase are plotted on a log scale for kinase alone (blue), in Nanodisc-based, single core complexes assembled with Tar-QEQE (green) or in those complexes in the presence of a near-saturating concentration of the Tar attractant ligand aspartate (red). For numerical values shown in (A) see Table I, for (B) see (Li & Hazelbauer, 2011b). A. Normalized k_{cat} values for phosphorylation of liberated CheA P1 by CheA P3-P4-P5. B. Normalized initial rate values for coupled phosphorylation of CheY by intact CheA.

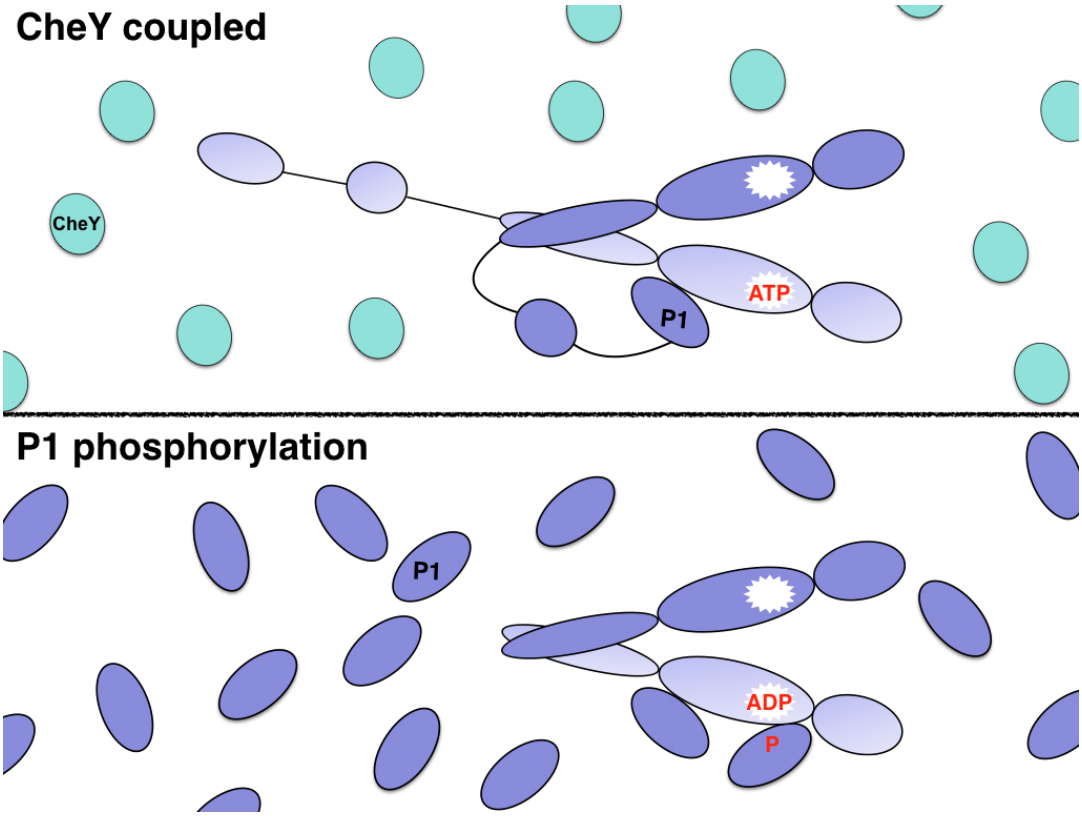

Fig. 20. Cartoons showing the difference between CheY coupled phosphorelay and P1 phosphorylation. Upper panel shows the CheY coupled assay. The intact CheA in this assay is shown in purple and CheY in cyan. The interaction between one of the tethered P1 domains and the P4 domain from the partner unit illustrates the alternative binding. Lower panel shows the P1 phosphorylation by P3-P4-P5 catalytic fragment. In this assay, free P1 domain is in much excess to the kinase. Even if P1 is sequestered by the alternative binding site on P4 domain, the great majority of P1 is still available for phosphorylation, which is not the case for CheY coupled assay with intact CheA.

Although simple sequestration of P1 cannot be a major contributor to kinase control, a P1-binding site distinct from the active site might be involved if occupancy of such a distinct, high-affinity site blocked access to the active site or disrupted it allosterically, and the inhibiting P1-binding site were available in the inactive state of the enzyme and but not in its active state. Thus transitions from inactive to active or vice versa would involve reductions or increases, respectively, in the proportion of the enzyme population with the inhibiting site available, generating apparent changes in k_{cat} values and little change in values of K_M.

K_M values for ATP and P1 are appropriate for their respective physiological concentrations

K_M values are generally related to the physiological concentrations of the respective substrates. This is the case for the chemotaxis kinase. The intracellular concentration of ATP in *E. coli* averages ~1.5 mM (Yaginuma et al., 2014). Most K_M values for ATP we determined ranged from 0.3 to 0.6 mM (Table I). Thus, in terms of ATP, autophosphorylation would proceed at 71 to 83% of maximal rate and the modest changes we observed for K_M^{ATP} values would affect the rate no more than ~20%. For P1, the relevant concentration for intact enzyme is the local concentration of the natively tethered domain. This concentration can be estimated as ~730 μM (see Materials and Methods). K_M^{P1} values ranged from ~100 to 430 μM, below the substrate concentration, but sufficiently close to allow modest effects on reaction rate. The largest change we observed for the P1 K_M, a shift from 430 μM for free kinase to 130 μM for kinase in isolated core complexes, would increase reaction rate ~20%.

A common target for kinase control by different inputs

Our understanding of interactions in signaling complexes is consistent with a common target for all three inputs that alter kinase activity. In signaling complexes, the enzyme has physical contact with chemoreceptors and CheW (Briegel et al., 2012; Liu et al., 2012; Cassidy et al., 2015) and thus kinase activation by formation of signaling complexes must involve one or both of these contacts. The magnitude of activation is a function of receptor signaling state. In signaling complexes, k_{cat} and k_{cat}/K_M of the kinase are enhanced relative to the free enzyme, but the magnitude is a function of the signaling state of the chemoreceptors in those complexes (Fig. 18). Tar-EEEE, strongly shifted to the "kinase-off" conformation, enhanced k_{cat} and k_{cat}/K_M only ~3-fold and ~10-fold, respectively. Tar-QQQQ, strongly shifted to the "kinase-on" conformation, enhanced k_{cat} and k_{cat}/K_M 470-fold and ~1000- fold, respectively (Table III). Shifting either conformation toward a kinase-off state by ligand occupancy reduced activation, for Tar-EEEE to the low activity of free CheA (Table III). A unified interpretation is that kinase activation by interaction with receptors in signaling complexes, whether by direct contact or via CheW, is a function of receptor signaling state, whether influenced by ligand occupancy or adaptational modification. Thus we suggest that all three inputs influence the kinase via the same physical contacts and in large part alter the same enzymatic property, the apparent kinase catalytic constant.

Materials and Methods

Plasmids, strains, proteins and Nanodiscs

Membrane scaffold protein MSP1D1E3(-) (Denisov et al., 2004) and CheW (Barnakov et al., 1998) were produced and purified as described. *Escherichia coli* Tar-EEEE, Tar-QEQE and Tar-QQQQ with six-histidine, carboxyl-terminal extensions were produced in *E. coli* K12 strain RP3098, which does not contain chemotaxis or chemoreceptor proteins (Parkinson & Houts, 1982), harboring pAL529 (Amin & Hazelbauer, 2010a), pAL67 (Lai & Hazelbauer, 2005) or pAL533 (Amin & Hazelbauer, 2010b), respectively. Cytoplasmic membranes enriched in the respective receptor forms were prepared as described (Boldog et al., 2007; Amin & Hazelbauer, 2010b). Nanodiscs containing 3.5 to 4 Tar dimers per disc were prepared using Ni-NTA affinity chromatography and size-exclusion chromatography (Li & Hazelbauer, 2011a). The P1 and the P3-P4-P5 fragment of *E. coli* CheA were isolated from *E. coli* BL21 (DE3) harboring pET28a carrying the coding sequence for CheA residues 1-134 with six histidines at its carboxyl terminus or for CheA residues 261-654 with the coding sequence for the amino-terminal six-histidine tag removed by mutagenic primers and PCR, respectively (Mo et al., 2012). Plasmid-harboring strains were inoculated into LB broth (10 g/L Bacto tryptone, 5 g/L Yeast extract, 10 g/L NaCl) at OD_{560} ~0.05, incubated with agitation at 35^{o}, IPTG (isopropyl β-D-1-thiogalactopyranoside) added at OD_{560} ~0.4 to induce expression and harvested at OD_{560} ~3.0. Cells were pelleted by centrifugation at 15,000 x g and 4^{o} in a SLC-6000 rotor (Thermo Fisher Scientific, Waltham, MA), suspended in a smaller volume of 50 mM Tris-HCl (pH 7.5), 0.5 mM EDTA, 2 mM dithiothreitol and 20% glycerol and lysed in a French Press at 4^{o}. Lysates were centrifuged at 100,000 x g and 4^{o} in a TL100.4 rotor

(Beckman Coulter, Brea, CA). Supernatants containing P1- His_6 were applied to a Ni-NTA column (GE Healthcare, Chicago, IL). The column was washed with 50 mM Tris-HCl (pH 7.5), 100 mM NaCl, 30 mM imidazole, 1 mM dithiothreitol, P1- His_6 eluded by 300 mM imidazole in the same buffer and fractions containing that protein pooled and dialyzed against 50 mM Tris-HCl (pH 7.5), 100 mM NaCl, 0.5 mM EDTA (ethylenediaminetetraacetic acid) and 2 mM dithiothreitol (TNED). Supernatants containing CheA P3-P4-P5 were applied to the QAE ion-exchange column Shodex QA-825 (Showa Denko, Tokyo, Japan) attached to an HPLC system (Gilson, Middleton, WI), a gradient of 0 to 0.8 M NaCl in 50 mM Tris-HCl (pH 7.5) applied and selected fractions containing P3-P4-P5 and minimal contaminants pooled and dialyzed against TNED. Protein concentrations were determined by quantitative immunoblots using purified standards for the respective proteins with concentrations determined by quantitative amino acid analysis.

Quantitative Immunoblotting

Concentration of P3-P4-P5 bound to signaling complexes is quantified by immunoblots. Samples were run on a standard SDS-PAGE gel. Protein was transferred from the gel to a nitrocellulose blotting membrane (pore size: 0.45 μm) for 1.5h at 12 V. The membrane was immersed in powdered milk, 2% in 20 mM Tris, pH 7.0, 0.5 M NaCl (PM-TBS) and placed on a shaker at 35 °C for 15 min. Then, the membrane was incubated with a rabbit antiserum, raised against purified CheA, at a dilution of 1:2000 in PM-TBS on a shaker at 35 °C overnight. After washing with TWEEN, 0.05 % (vol/vol)) in PM-TBS for 15 min, the membrane was immersed in a 1:2000 dilution of the secondary antibody that is a goat

antiserum raised against rabbit immunoglobulin G and conjugated with horseradish peroxidase. The washing step was repeated, and the blot was developed with a solution of 4-chloro-1-napthol created by dissolving 15 mg in 5 ml of methanol, mixing with 25 ml TBS and adding 15 µl of 30 % H_2O_2 immediately before use. The membranes were photographed using a KODAK EDAS 290 digital camera system. The intensity of the bands was quantified using TotalLab. The amount of P3-P4-P5 was calculated from the intensity of each band using a standard curve of pure P3-P4-P5 present on the same blot.

Signaling complexes

Mixtures of 5 µM CheW, 2 µM P3-P4-P5 and 10 µM chemoreceptor Tar-6H in different modification states, inserted in Nanodiscs or in native membrane vesicles, were incubated and processed as described (Li & Hazelbauer, 2011a, 2014). For Nanodisc-based core complexes, the resulting signaling complexes were separated from free P3-P4-P5 with a Ni-NTA column (Li & Hazelbauer, 2011a, 2014). For native-membrane-based small arrays of core complexes, separation was performed by two rounds of centrifugation and suspension in a solution with no P3-P4-P5 (Erbse & Falke, 2009). Amounts of P3-P4-P5 incorporated into signaling complexes were determined by quantitative immunoblotting as described above.

Kinase assays

Kinase activity was assayed essentially as described (Li & Hazelbauer, 2011a). P3-P4-P5 alone (2 µM) or in signaling complexes (varies in the range of 0.02 – 0.04 µM for core signaling complexes, 0.2 – 0.4 µM for small arrays) was incubated 15 min at room temperature in TNED plus 50 mM KCl and 5 mM MgCl2 without or with aspartate.

Reactions were initiated by addition of [γ-^{32}P] ATP and terminated by addition of 4X SDS sample buffer (80 mM Tris, 32 mM NaH_2PO_4, pH 7.8, 4% (w/v) SDS, 80 mM dithiothreitol, 20 mM EDTA, 0.012% (w/v) Bromphenol Blue, 40% (w/v) glycerol) containing 20 mM EDTA at 15 s for Tar-QEQE and Tar-QQQQ or 60 s for Tar- EEEE (Fig. 12). Samples were applied to a SDS-PAGE gel and ^{32}P-P1 quantified by phosphorimaging and Image Gauge analysis software.

Calculating k_{cat}

Apparent catalytic constants determined by varying one substrate (ATP or P1) with the other substrate (P1 or ATP) constant at a sub-saturating concentration were necessarily lower than k_{cat}, the turnover number of the kinase at saturation for both substrates. The Michaelis–Menten equation was used to calculate k_{cat} values at saturation of both substrates from each apparent catalytic constant determined experimentally (Those values are shown in the figures and tables, and cited in the text.). For example, for kinase in core complex, the K_M^{ATP} (determined when ATP concentration is varied) is 477 μM. When P1 concentration is varied at a constant 1000 μM ATP, the k_{cat} determined is 1.9 s^{-1}. Referring to the Michaelis–Menten equation $v = \frac{V_{max}[S]}{K_M+[S]}$, if K_M is 477 μM and [S] is 1000 μM. V_{max} (when the concentration of ATP is at saturation)/v (at 1000 μM ATP) is 1.48. Thus the k_{cat} when P1 concentration is varied at saturating ATP concentration should be 1.48 times higher than 1.9 μM, which is 2.8 μM (Table 1).

Local concentration of tethered P1 for intact CheA

Following the lead of Greenswag et al. (Greenswag et al., 2015) we calculated an approximate operational concentration of tethered P1 in intact CheA by assuming a

Gaussian chain model and utilizing the Jacobson-Stockmayer factor, which estimates the concentration of one end of a flexible chain in the vicinity of the other. That factor is:

$$j = \left(\frac{3}{2\pi * C_n * n * l^2}\right)^{3/2}$$

where C_n is the Flory characteristic ratio, n the number of links in the chain and l the chain unit length. Using the poly-L-alanine C_n of 9.5, n = 60 which represents the sum of residues in the P1-P2 and P2-P3 linkers plus one residue distance between the position of the N- and C- termini of P2, and 3.8 Å for the unit length, we calculated an estimated operational concentration of tethered P1 of ~730 μM.

CHAPTER THREE

Additional considerations of CheA Kinetics

Special considerations for measurements of the activity of CheA alone

In considering the activity of P3P4P5 alone, two issues arose. First, CheA is in an equilibrium between an inactive monomeric form and an active dimeric form. Secondly, its activity is so slow that whether steady-state is achieved in a few minutes needs to be explored. For the first consideration, we were interested in determining the equilibrium constant K_{eq} for CheA P3P4P5 in our own experimental conditions. The K_{eq} would help us calculate how much P3P4P5 was in the active dimeric form in kinase assays in order to get a more accurate k_{cat} value which was calculated by dividing rate with kinase concentration. We planned to follow the procedure of Surette et al. (Surette et al., 1996) and determine the K_{eq} by measuring activities obtained from timecourses as a function of total kinase concentration. For the second consideration, we were interested in seeing a full reaction progress rather than the very beginning of the phosphorylation timecourse (Fig. 21). Thus we did a much longer timecouse (Fig. 22). We were surprised to see that the linear steady-state phase actually occurred much later in the timecourse after a burst phase in a scale of minutes, which usually takes place within milliseconds for most enzymes. This indicates that using 60 s as sampling time for the steady-state study described in Chapter two was not accurate, since the rate in the first minute of the burst phase (Fig. 22) is many fold higher than the rate of the steady-state phase. As a result, we overestimated the activity of CheA P3P4P5 alone.

To address the above two issues, we proceeded to do a series of long timecourses for CheA P3P4P5 in different concentrations in order to get at the same time the K_{eq} and the k_{cat} value when all kinase is in dimeric form.

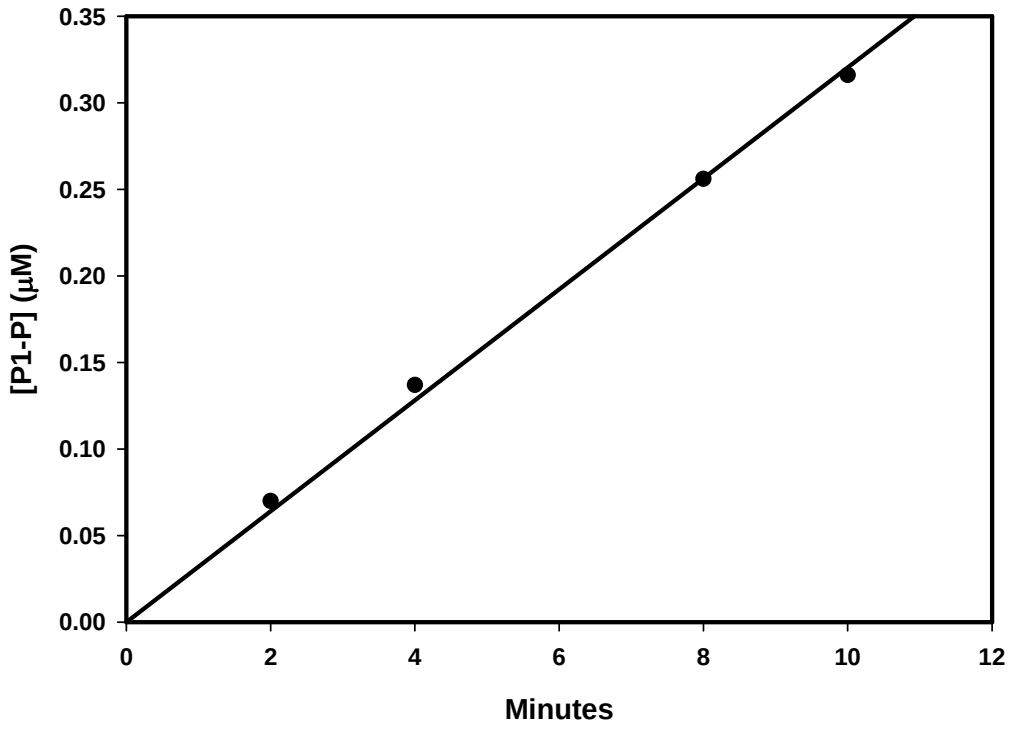

Fig. 21. Timecourse for P1 phosphorylation by P3P4P5 alone. This is the initial timecourse that shows the beginning of the reaction progress. Points are fit to a linear line that goes through origin. It was used to determine sampling time (60 s) for steady-state study of the kinase. Experiment follows the basic kinase assay procedure (see Materials and Methods in Chapter two). The concentration of P1 is 180 μM, ATP 1000 μM, P3P4P5 0.9 μM.

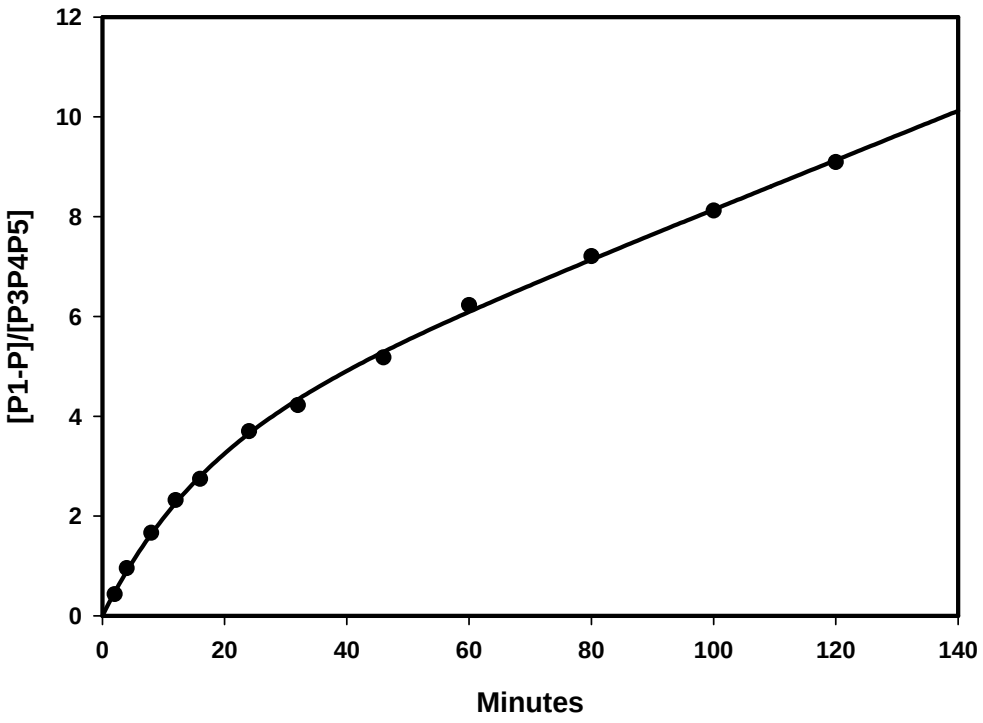

Fig. 22. Timecourse for P1 phosphorylation by P3P4P5. This is a longer timecourse that shows a pre-steady burst followed by steady-state turnover. Points are fit to the equation shown in text. Experiment follows the basic kinase assay procedure (see Materials and Methods in Chapter two). The concentration of P1 is 100 μM, ATP 1000 μM, P3P4P5 1 μM.

A total of five concentrations of P3P4P5 were done for the timecourses (Fig. 23). They are fit to an equation representing transient-state reaction that has a presteady-state burst followed by steady-state turnover at a rate given by k_{app} (Johnson, 1992):

$$f = A(1 - e^{-bt}) + k_{app}t$$

where A, b and k_{app} are functions of the rate constants involved in the reaction pathway. The k_{app} values corresponding to different P3P4P5 concentrations are plotted in Fig. 24. The data points are fit to a standard hyperbolic equation:

$$k_{app} = \frac{k_{max}[P3P4P5]}{K_{eq}+[P3P4P5]}$$

The maximum k_{app}, k_{max}, which is the k_{cat} for P3P4P5 alone when all kinase is in the dimeric form, is 0.056 min^{-1} or 0.001 s^{-1}, 10-fold lower than the previous value 0.01 s^{-1} we determined in Chapter two. This means kinase activation by formation of signaling complexes is much more dramatic (~ 3000-fold) than that we indicated (~ 300-fold) in Chapter two. The K_{eq} determined for P3P4P5 here, 0.29 μM, is in the range of the numbers from Stock lab's papers for full-length CheA (0.2-0.4 μM) (M. Levit et al., 1996) and CheA catalytic fragment P3P4P5 (0.2 μM) (Levit et al., 1996; Surette et al., 1996). This finding once again proves that P1 and P2 domains don't contribute to the dimerization of the kinase.

The work described in this section helped us obtain a more accurate k_{cat} for P3P4P5 alone, which strengthens our observation about activation by formation of signaling complexes. The K_{eq} determined in the process is informative and useful for future experiments to determine the proportion of active dimeric CheA for a given total concentration of the kinase.

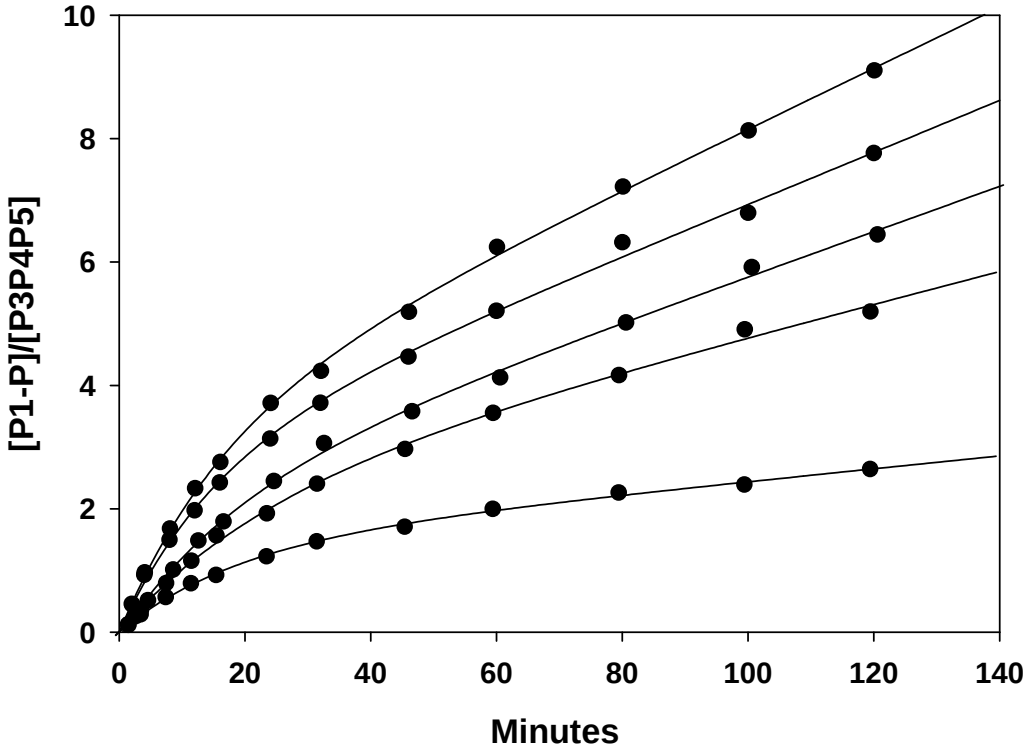

Fig. 23. Timecourses for P1 phosphorylation by CheA P3-P4-P5 at different concentrations. The data for P1 phosphorylation at five different concentrations of P3P4P5 were fit to an equation for transient state kinetics. From the top to bottom the P3-P4-P5 concentrations are: 2 μM, 1 μM, 0.5 μM, 0.2 μM, 0.1 μM. For all experiments, the concentration of P1 is 100 μM, ATP 1000 μM. k_{app} values from the top to bottom are: 0.10 min^{-1}, 0.026 min^{-1}, 0.036 min^{-1}, 0.042 min^{-1}, 0.049 min^{-1}.

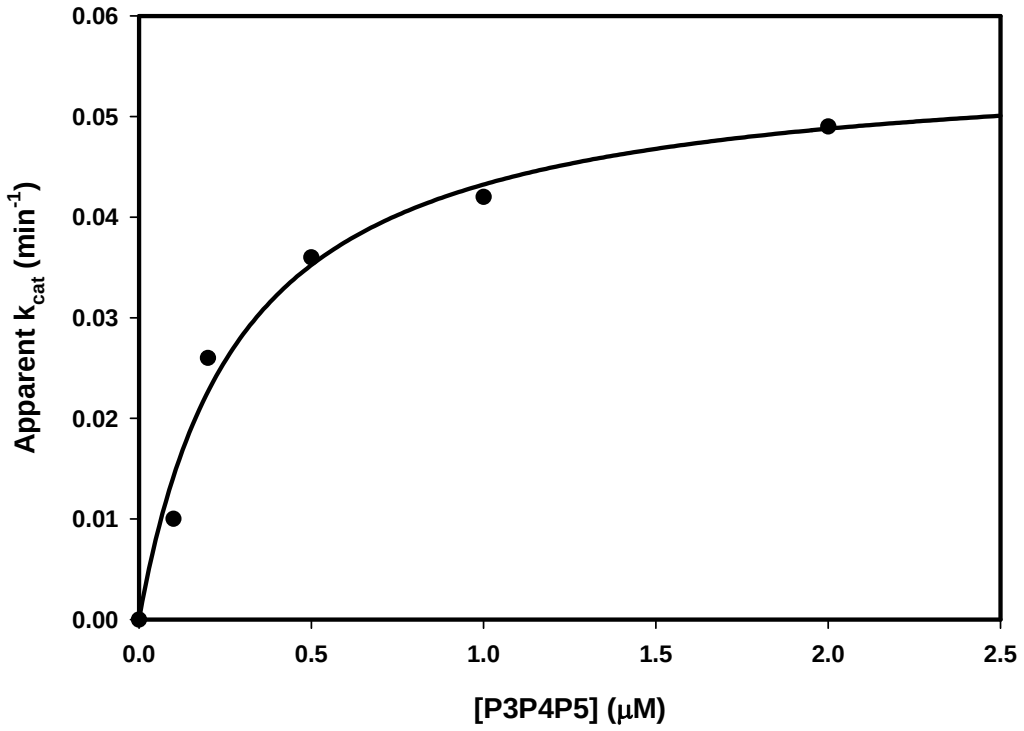

Fig. 24. The correlation between the apparent k_{cat} and [P3-P4-P5]. The data points are fit to a standard hyperbolic equation: $\boldsymbol{Apparent\ k_{cat}} = \frac{k_{max}[P3P4P5]}{K_{eq}+[P3P4P5]}$. The maximum apparent k_{cat} is 0.056 min^{-1}. At half of its value, the total concentration of P3P4P5 that equals to K_{eq} is 0.29 μM.

Controlling kinase CheA activity

The work described in Chapter two has ruled out a simple sequestration mechanism for P1 domain to control the activity of CheA. Our finding suggested that the effects of complex formation, ligand binding and receptor modification were on the kinase active site or on an equilibrium between an active and inactive state of the kinase. To explore these two alternatives, we can consider these two scenarios: 1) The signals received by CheA from receptors during those signaling events alter the active site of CheA in a way that does not have much effect on the binding between either of the two substrates (P1 and ATP) and the active site of CheA, but affects the binding between the transition states of the substrates and the residues at the active site of CheA, thus affects the catalysis (k_{cat}). 2) The signals CheA receives can alter the equilibrium between an inactive form and an active form of CheA.

If scenario 1) were the case, here are some potential candidates. Site-directed mutagenesis of the key residues around the active site of CheA (Fig. 25) resulted in inactive kinases. Only half of them had detectable activities. Among these impeded kinases, the mutations primarily affected the k_{cat}, not the K_M of ATP (Fig. 25 and Table IV) (Hirschman et al., 2001). This argues for the possibility that the key residues at the active site of CheA are responsible for different functions (interacting with the substrates or interacting with the transition states or both). The fact that we observed similar outcomes in terms of k_{cat} and K_M for ATP could be because the signals (ligand binding, receptor modification) modulate the conformation of CheA P4 domain and prompt similar effects on these residues as those mutations. The effect could be on one or more of those key residues and alter the k_{cat} and K_M to different extent.

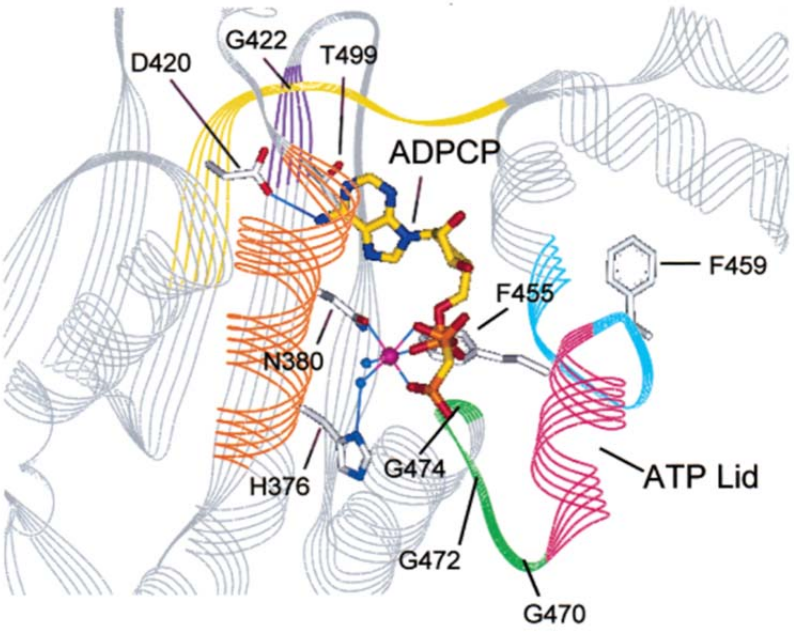

Fig. 25. Active site on P4 in complex with ADPCP, adapted from (Hirschman et al., 2001). CheA P4 domain is shown in ribbon with ATP-lid in pink. Residues at the active site are labelled, some of which shown as ball-and-stick. ATP analog ADPCP (5'-adenosyl-methylene-triphosphate) at the active site is shown as ball-and-stick.

Also, the other part that completes the active site, the P1 domain, can potentially be regulated. The residue Glu70 on P1 has been shown to be important for phosphorylation (Quezada et al., 2004). With the help of Lys51 and His67, Glu70 forms a hydrogen-bonding network with the phosphor-receiver His48, stabilizing the energetically unfavored $N^{\delta 1}H$ tautomer of His48 (Fig. 26 and Table IV) (Quezada et al., 2005). This makes the $N^{\varepsilon 2}$ of His48 unprotonated and well positioned to attack the γ-phosphate of ATP (Quezada et al., 2005). Although there is no direct evidence that these residues are regulated during signaling, it is possible for them to be involved in the regulation of the active site in a way that disturbs the interaction between these residues and the residues at the active site.

If scenario 2) were true, where an equilibrium between an active kinase and an inactive kinase exists, two observations suggest interactions that could be involved. First, computer simulations of signaling complex using the structure from EM tomography have suggested two conformations of CheA in signaling complexes (Cassidy et al., 2015). The difference between these two conformations is essentially in the position of P4 domain relative to the receptors. The active site on P4 can potentially be blocked (closed) by receptors in one of the two conformations and is exposed (open) in the other (Fig. 27). The electrostatic interactions between R265, D272 from P3 domain and K364, E368, D372 from P4 domain maintain the "open" conformation (Fig. 27 and Table IV). Germán E. Piñas in Sandy Parkinson's lab (unpublished data) showed that CheA with single mutations at these individual residues that disrupted interactions involved in "open" conformation could result in inability of kinase to be activated by formation of

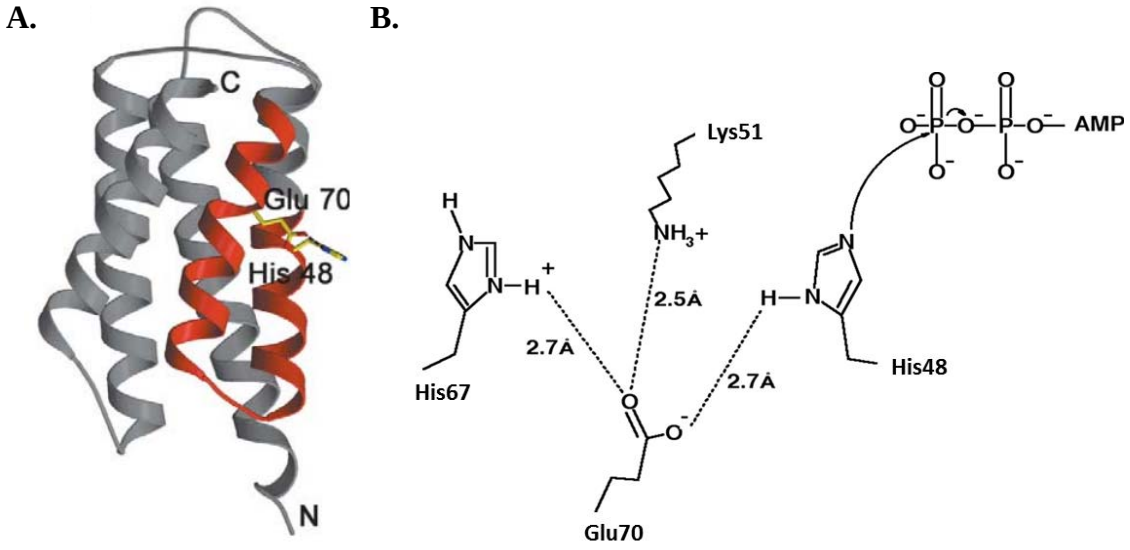

Fig. 26. P1 domain and the hydrogen-bonding network at His48. A. CheA P1 domain shown in ribbon with Glu70 and His48 in ball-and-stick, adapted from (Quezada et al., 2004). B. Hydogen bonding between Glu70 and His48 with the help of Lys51 and His67, adapted from (Quezada et al., 2005).

Table IV. *E. coli* CheA-key-residue mutations summary

Domain	Mutation	Activity (CheA alone) relative to WT	Note	Reference
P1	K51A	< 10%	These residues are involved in the hydrogen- bonding network surrounding His-48 that optimizes phosphotransfer.	Quezada et al., 2005
P1	H67A	< 10%		
P1	E70Q/D/A	< 10%		
P4	D363R	< 10%	K364, E368 and D372 are residues responsible for interactions with R265 and D272 on P3 domain to maintain the "open" conformation of CheA P4 in complex.	Wang et al., 2014
P4	K364D	< 10%		
P4	E368R	20%		
P4	R369D	20%		
P4	D372R	< 10%		
P4	H376Q	4%	These are conserved residues localized in the N, G1, F, G2 boxes that define the ATP binding pocket. The effects of these mutations on ATP binding are much less significant than on the catalytic activity, which echoes with our results.	Hirschman et al., 2001
P4	N380D	< 1%		
P4	D420N	< 1%		
P4	D420E	10%		
P4	G422A	< 1%		
P4	F455Y	< 2%		
P4	F459Y	< 2%		
P4	G470A	< 1%		
P4	G472A	< 1%		
P4	G474A	< 1%		

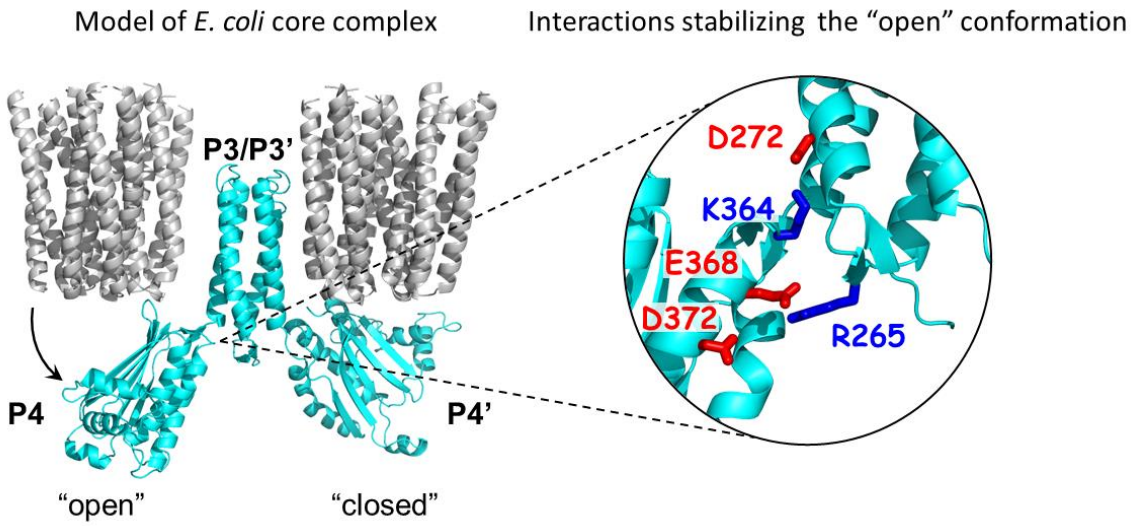

Fig. 27. Two conformations of CheA P4 in signaling complex proposed by computer simulations (Cassidy et al., 2015). Left panel shows the signaling complex in ribbon. For clarity, CheW is not shown and only the regulatory region of receptors and the P3P4 domains of CheA are shown. Right panel shows a blow-up of the interface between P3 and P4 domain. Residues responsible for stabilizing the "open" conformation are labeled.

signaling complexes. They proposed a model that in the "closed" conformation of CheA, the active site on P4 is blocked by receptors, thus it cannot be activated. This equilibrium between the "open"and "closed" conformations of CheA could be affected by the signaling events.In contrast to the first consideration, where the active site on P4 does not change by itself, the second consideration involves the conformational change at the active site, particularly with the ATP-lid. The ATP-lid of P4 is composed of the flexible loop between α2 and α3 (Fig. 28). This region is poorly resolved in crystal structures when P4 is free from nucleotide binding, but is resolved with nucleotide at the binding pocket (Bilwes et al., 2001). As is shown in Fig. 28, in the P4-ADPCP-Mg^{2+} complex, the ATP-lid forms a helix structure that borders the nucleotide-binding cavity, exposing the γ-phosphate of ATP and creating the dimensions that are appropriate for binding P1. Based on this crystal structure, Zhang et al. built a structural model for P4-ATP (Zhang et al., 2005). The molecular dynamics simulations on the P4-ATP complex suggested that upon ATP binding, the nucleotide forms hydrogen bonds with His413 (*Thermotoga maritima*) and Lys494 (*T. maritima*) near the active site (Zhang et al., 2005). But then ATP changes its conformation to one with lower energy, which ruptures the hydrogen bonding. As a consequence, Lys494 moves away from the active site, leading to the opening of the ATP-lid (open state). P1 can then bind to this open state tightly (Zhang et al., 2005) for phosphorylation. Signaling events can affect an equilibrium between an active state and an inactive state of the ATP-lid, thus affect the activity of CheA.

We were interested in the mutagenesis data of Parkinson lab mentioned above on the residues R265, D272 from P3 domain and K364, E368, D372 from P4 domain, the interactions among which maintain the "open" conformation in which the kinase is active

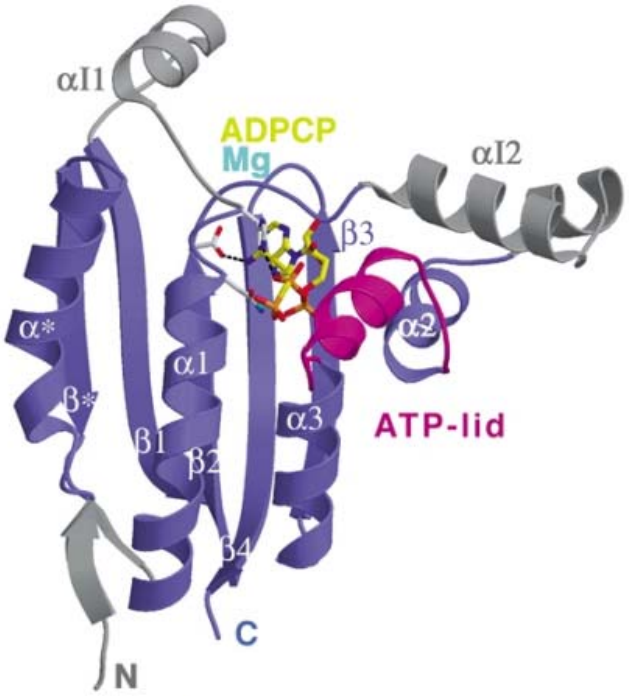

Fig. 28. P4-ADPCP-Mg^{2+} complex, adapted from (Bilwes et al., 2001). CheA P4 domain is shown as a ribbon diagram with the ATP-lid shown in pink. ATP analog ADPCP at the active site is shown in ball-and-stick model.

in signaling complex. We did kinase assays on CheA P3P4P5-D272R alone and in signaling complexes (Fig. 29). Our preliminary data showed that this mutant had a much lower basal (kinase alone) activity than the wildtype P3P4P5 and was not activated as much (~ 3-fold) in signaling complexes as was the wildtype (which is dramatically activated more than 300-fold in signaling complexes as described in Chapter two and more than 3000-fold comparing with the k_{cat} determined in the first section of Chapter three). It was interesting to find that this low activity of the mutant in signaling complexes was further reduced significantly (~ 40-fold) when applying ligands to the complexes. Altogether, these data argue that activation by signaling complex formation and inhibition by ligand binding may involve different residues on CheA, i.e. activation and inhibition are not symmetric. Further experiments with other mutants will be done to study this observation.

Although the mechanism of control of CheA kinase activity is still not clear, the biochemical experiments, molecular dynamic simulations and crystal structures of CheA described above from a number of labs have provided enlightening information about this subject. The two states of CheA in signaling complexes proposed by Keith Cassidy and colleagues (Cassidy et al., 2015) based on computer simulations provides a simple way of control – an equilibrium between "kinase-off" and "kinase-on" that can be altered by signaling events such as ligand binding and receptor modification. However, this idea does not seem to address how the kinase is activated dramatically upon signaling complex formation. If blocking and unblocking of the active site on P4 by receptors were the mechanisms of kinase activity control, why does the kinase alone have so little activity when there are no receptors around to block its active site? Thus an alteration of

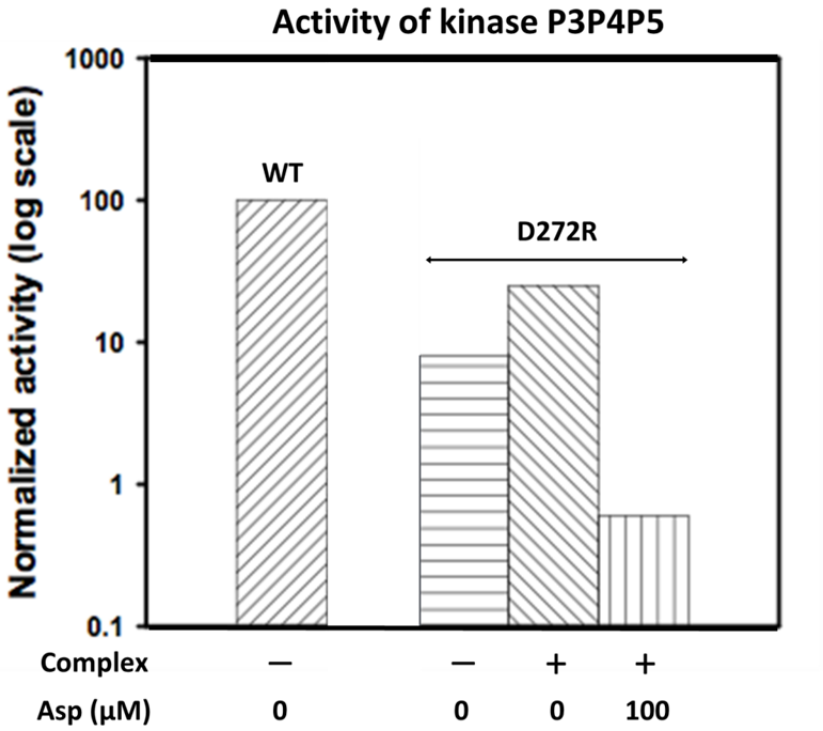

Fig. 29. Preliminary data on P3P4P5 D272R. Activities of kinase P3P4P5 wildtype (WT) and D272R are obtained as k_{app} values from timecourses and normalized to the activity of wildtype P3P4P5 alone. k_{app} values are: WT P3P4P5 alone, 0.056 min^{-1}; P3P4P5 D272R alone, 0.0045 min^{-1}; P3P4P5 D272R in complex, 0.014 min^{-1}; P3P4P5 D272R in complex plus 100 μM Asp, 0.00034 min^{-1}.

the intrinsic catalytic activity of the kinase seems more likely to be involved during signaling. This alteration could mean the conformational change of CheA P4 domain, particularly at the active site, affecting the ATP-lid, the proper position of which helps the process of phosphorylation (Zhang et al., 2005) (Bilwes et al., 2001), as well as the crucial residues (Hirschman et al., 2001) distributed around the active site. Thus our data could be reflecting these altered activities.

LITERATURE CITED

Aiba, H., & Mizuno, T. (1990). Phosphorylation of a bacterial activator protein, OmpR, by a protein kinase, EnvZ, stimulates the transcription of the *ompF* and *ompC* genes in *Escherichia coli*. *FEBS Lett, 261*(1), 19-22.

Alon, U., Surette, M. G., Barkai, N., & Leibler, S. (1999). Robustness in bacterial chemotaxis. *Nature, 397*(6715), 168-171.

Amin, D. N., & Hazelbauer, G. L. (2010a). The chemoreceptor dimer is the unit of conformational coupling and transmembrane signaling. *Journal of Bacteriology, 192*(5), 1193-1200. doi: 10.1128/jb.01391-09

Amin, D. N., & Hazelbauer, G. L. (2010b). Chemoreceptors in signalling complexes: shifted conformation and asymmetric coupling. *Molecular Microbiology, 78*(5), 1313-1323. doi: 10.1111/j.1365-2958.2010.07408.x

Anand, G. S., Goudreau, P. N., & Stock, A. M. (1998). Activation of Methylesterase CheB: Evidence of a Dual Role for the Regulatory Domain. *Biochemistry, 37*(40), 14038-14047. doi: 10.1021/bi980865d

Anand, G. S., & Stock, A. M. (2002). Kinetic Basis for the Stimulatory Effect of Phosphorylation on the Methylesterase Activity of CheB. *Biochemistry, 41*(21), 6752-6760. doi: 10.1021/bi012102n

Baker, M. D., Wolanin, P. M., & Stock, J. B. (2006). Signal transduction in bacterial chemotaxis. *Bioessays, 28*(1), 9-22.

Ban, C., & Yang, W. (1998). Crystal Structure and ATPase Activity of MutL. *Cell, 95*(4), 541-552.

Barnakov, A. N., Barnakova, L. A., & Hazelbauer, G. L. (1998). Comparison in vitro of a high- and a low-abundance chemoreceptor of *Escherichia coli*: similar kinase activation but different methyl-accepting activities. *Journal of Bacteriology, 180*(24), 6713-6718.

Berg, H. C. (2000). Motile behavior of bacteria. *Physics Today, 53*((1)), 24-29.

Bilwes, A. M., Alex, L. A., Crane, B. R., & Simon, M. I. (1999). Structure of CheA, a signal-transducing histidine kinase. *Cell, 96*(1), 131-141.

Bilwes, A. M., Quezada, C. M., Croal, L. R., Crane, B. R., & Simon, M. I. (2001). Nucleotide binding by the histidine kinase CheA. *Nat Struct Biol, 8*(4), 353-360.

Block, S. M., Segall, J. E., & Berg, H. C. (1982). Impulse responses in bacterial chemotaxis. *Cell, 31*(1), 215-226.

Boldog, T., Grimme, S., Li, M., Sligar, S. G., & Hazelbauer, G. L. (2006). Nanodiscs separate chemoreceptor oligomeric states and reveal their signaling properties. *Proceedings of the National Academy of Sciences of the United States of America, 103*(31), 11509-11514.

Boldog, T., Li, M., & Hazelbauer, G. L. (2007). Using Nanodiscs to create water-soluble transmembrane chemoreceptors inserted in lipid bilayers. *Methods in Enzymology, 423*, 317-335.

Borkovich, K. A., Alex, L. A., & Simon, M. I. (1992). Attenuation of sensory receptor signaling by covalent modification. *Proceedings of the National Academy of Sciences of the United States of America, 89*(15), 6756-6760.

Borkovich, K. A., Kaplan, N., Hess, J. F., & Simon, M. I. (1989). Transmembrane signal transduction in bacterial chemotaxis involves ligand-dependent activation of phosphate group transfer. *Proceedings of the National Academy of Sciences of the United States of America, 86*(4), 1208-1212.

Borkovich, K. A., & Simon, M. I. (1990). The dynamics of protein phosphorylation in bacterial chemotaxis. *Cell, 63*(6), 1339-1348.

Bornhorst, J. A., & Falke, J. J. (2001). Evidence that both ligand binding and covalent adaptation drive a two-state equilibrium in the aspartate receptor signaling complex. *Journal of General Physiology, 118*(6), 693-710.

Bourret, R. B., Hess, J. F., Borkovich, K. A., Pakula, A. A., & Simon, M. I. (1989). Protein phosphorylation in chemotaxis and two-component regulatory systems of bacteria. *Journal of Biological Chemistry, 264*(13), 7085-7088.

Bren, A., & Eisenbach, M. (2000). How signals are heard during bacterial chemotaxis: protein-protein interactions in sensory signal propagation. *Journal of Bacteriology, 182*(24), 6865-6873.

Briegel, A., Ames, P., Gumbart, J. C., Oikonomou, C. M., Parkinson, J. S., & Jensen, G. J. (2013). The mobility of two kinase domains in the *Escherichia coli* chemoreceptor array varies with signalling state. *Molecular Microbiology, 89*(5), 831-841. doi: 10.1111/mmi.12309

Briegel, A., Li, X., Bilwes, A. M., Hughes, K. T., Jensen, G. J., & Crane, B. R. (2012). Bacterial chemoreceptor arrays are hexagonally packed trimers of receptor dimers networked by rings of kinase and coupling proteins. *Proceedings of the National Academy of Sciences of the United States of America, 109*(10), 3766-3771. doi: 10.1073/pnas.1115719109

Briegel, A., Wong, M. L., Hodges, H. L., Oikonomou, C. M., Piasta, K. N., Harris, M. J., Fowler, D. J., Thompson, L. K., Falke, J. J., Kiessling, L. L., & Jensen, G. J. (2014). New insights into bacterial chemoreceptor array structure and assembly from electron cryotomography. *Biochemistry, 53*(10), 1575-1585. doi: 10.1021/bi5000614

Cassidy, C. K., Himes, B. A., Alvarez, F. J., Ma, J., Zhao, G., Perilla, J. R., Schulten, K., & Zhang, P. (2015). CryoEM and computer simulations reveal a novel kinase conformational switch in bacterial chemotaxis signaling. *eLife, 4*, e08419. doi: 10.7554/eLife.08419

Denisov, I. G., Grinkova, Y. V., Lazarides, A. A., & Sligar, S. G. (2004). Directed self-assembly of monodisperse phospholipid bilayer nanodiscs with controlled size. *Journal of the American Chemical Society, 126*(11), 3477-3487.

Djordjevic, S., Goudreau, P. N., Xu, Q., Stock, A. M., & West, A. H. (1998). Structural basis for methylesterase CheB regulation by a phosphorylation-activated domain. *Proc. Natl. Acad. Sci. U.S.A., 95*(4), 1381-1386.

Djordjevic, S., & Stock, A. M. (1998). Chemotaxis receptor recognition by protein methyltransferase CheR. *Nat Struct Biol, 5*(6), 446-450.

Duke, T. A., & Bray, D. (1999). Heightened sensitivity of a lattice of membrane receptors. *PNAS, 96*(18), 10104-10108.

Dunten, P., & Koshland, D. E., Jr. (1991). Tuning the responsiveness of a sensory receptor via covalent modification. *Journal of Biological Chemistry, 266*(3), 1491-1496.

Dutta, R., Qin, L., & Inouye, M. (1999). Histidine kinases: diversity of domain organization. *Molecular Microbiology, 34*(4), 633-640. doi: 10.1046/j.1365-2958.1999.01646.x

Eisenbach, M. (1996). Control of bacterial chemotaxis. *Molecular Microbiology, 20*(5), 903-910.

Erbse, A. H., & Falke, J. J. (2009). The core signaling proteins of bacterial chemotaxis assemble to form an ultrastable complex. *Biochemistry, 48*(29), 6975-6987.

Falke, J. J., Bass, R. B., Butler, S. L., Chervitz, S. A., & Danielson, M. A. (1997). The two-component signaling pathway of bacterial chemotaxis: a molecular view of signal transduction by receptors, kinases, and adaptation enzymes. *Annual Review of Cell and Developmental Biology, 13*(52), 457-512.

Francis, N. R., Wolanin, P. M., Stock, J. B., DeRosier, D. J., & Thomas, D. R. (2004). Three-dimensional structure and organization of a receptor/signaling complex. *Proceedings of the National Academy of Sciences of the United States of America, 101*(50), 17480-17485.

Gao, R., & Stock, A. M. (2009). Biological insights from structures of two-component proteins. *Annual Review of Microbiology, 63*(1), 133-154.

Garzon, A., & Parkinson, J. S. (1996). Chemotactic signaling by the P1 phosphorylation domain liberated from the CheA histidine kinase of *Escherichia coli*. *Journal of Bacteriology, 178*(23), 6752-6758.

Gegner, J. A., & Dahlquist, F. W. (1991). Signal transduction in bacteria: CheW forms a reversible complex with the protein kinase CheA. *Proceedings of the National Academy of Sciences of the United States of America, 88*(3), 750-754.

Goh, B. C., Hadden, J. A., Bernardi, R. C., Singharoy, A., McGreevy, R., Rudack, T., Cassidy, K., & Schulten, K. (2016). Computational Methodologies for Real-Space

Structural Refinement of Large Macromolecular Complexes. *Annual Review of Biophysics, 45*, 253-278.

Greenswag, A. R., Muok, A., Li, X., & Crane, B. R. (2015). Conformational transitions that enable histidine kinase autophosphorylation and receptor array integration. *Journal of Molecular Biology, 427*(24), 3890-3907.

Griswold, I. J., Zhou, H., Matison, M., Swanson, R. V., McIntosh, L. P., Simon, M. I., & Dahlquist, F. W. (2002). The solution structure and interactions of CheW from *Thermotoga maritima*. *Nat Struct Biol, 9*(2), 121-125.

Hamel, D. J., Zhou, H., Starich, M. R., Byrd, R. A., & Dahlquist, F. W. (2006). Chemical-shift-perturbation mapping of the phosphotransfer and catalytic domain interaction in the histidine autokinase CheA from *Thermotoga maritima*. *Biochemistry, 45*(31), 9509-9517. doi: 10.1021/bi060798k

Hazelbauer, G. L., Falke, J. J., & Parkinson, J. S. (2008). Bacterial chemoreceptors: high-performance signaling in networked arrays. *Trends in Biochemical Sciences, 33*(1), 9-19. doi: 10.1016/j.tibs.2007.09.014

Hazelbauer, G. L., & Lai, W.-C. (2010). Bacterial chemoreceptors: providing enhanced features to two-component signaling. *Current Opinion in Microbiology, 13*(2), 124-132. doi: DOI: 10.1016/j.mib.2009.12.014

Hess, J. F., Oosawa, K., Kaplan, N., & Simon, M. I. (1988). Phosphorylation of three proteins in the signaling pathway of bacterial chemotaxis. *Cell, 53*(1), 79-87.

Hess, J. F., Oosawa, K., Matsumura, P., & Simon, M. I. (1987). Protein phosphorylation is involved in bacterial chemotaxis. *PNAS, 84*(21), 7609-7613.

Hirschman, A., Boukhvalova, M., VanBruggen, R., Wolfe, A. J., & Stewart, R. C. (2001). Active site mutations in CheA, the signal-transducing protein kinase of the chemotaxis system in *Escherichia coli*. *Biochemistry, 40*(46), 13876-13887.

Jahreis, K., Morrison, T. B., Garzón, A., & Parkinson, J. S. (2004). Chemotactic Signaling by an Escherichia coli CheA Mutant That Lacks the Binding Domain for Phosphoacceptor Partners. *Journal of Bacteriology, 186*(9), 2664-2672.

Johnson, K. A. (1992). Transient-state kinetic analysis of enzyme reaction pathways *The Enzymes* (3rd ed., Vol. XX, pp. 1-66). New York: Academic Press.

Kehry, M. R., & Dahlquist, F. W. (1982). Adaptation in bacterial chemotaxis: CheB-dependent modification permits additional methylations of sensory transducer proteins. *Cell, 29*(3), 761-772.

Kehry, M. R., Doak, T. G., & Dahlquist, F. W. (1985). Sensory adaptation in bacterial chemotaxis: regulation of demethylation. *Journal of Bacteriology, 163*(3), 983-990.

Kim, K. K., Yokota, H., & Kim, S.-H. (1999). Four-helical-bundle structure of the cytoplasmic domain of a serine chemotaxis receptor. *Nature, 400*(6746), 787-792.

Lai, R.-Z., Manson, J. M. B., Bormans, A. F., Draheim, R. R., Nguyen, N. T., & Manson, M. D. (2005). Cooperative signaling among bacterial chemoreceptors. *Biochemistry, 44*(43), 14298-14307.

Lai, W.-C., & Hazelbauer, G. L. (2005). Carboxyl-terminal extensions beyond the conserved pentapeptide reduce rates of chemoreceptor adaptational modification. *Journal of Bacteriology, 187*(15), 5115-5121.

Levit, M., Liu, Y., Surette, M., & Stock, J. (1996). Active site interference and asymmetric activation in the chemotaxis protein histidine kinase CheA. *Journal of Biological Chemistry, 271*(50), 32057-32063.

Levit, M. N., Liu, Y., & Stock, J. B. (1999). Mechanism of CheA protein kinase activation in receptor signaling complexes. *Biochemistry, 38*(20), 6651-6658.

Li, G., & Weis, R. M. (2000). Covalent modification regulates ligand binding to receptor complexes in the chemosensory system of *Escherichia coli*. *Cell, 100*(3), 357-365.

Li, J., Swanson, R. V., Simon, M. I., & Weis, R. M. (1995). The response regulators CheB and CheY exhibit competitive binding to the kinase CheA. *Biochemistry, 34*(45), 14626-14636.

Li, M., & Hazelbauer, G. L. (2005). Adaptational assistance in clusters of bacterial chemoreceptors. *Molecular Microbiology, 56*(6), 1617-1626.

Li, M., & Hazelbauer, G. L. (2011a). Core unit of chemotaxis signaling complexes. *Proceedings of the National Academy of Sciences of the United States of America, 108*(23), 9390-9395.

Li, M., & Hazelbauer, G. L. (2011b). Core unit of chemotaxis signaling complexes. *Proc. Natl. Acad. Sci. U.S.A., 108*(23), 9390-9395.

Li, M., & Hazelbauer, G. L. (2014). Selective allosteric coupling in core chemotaxis signaling complexes. *Proceedings of the National Academy of Sciences of the United States of America, 111*(45), 15940-15945. doi: 10.1073/pnas.1415184111

Li, X., Fleetwood, A. D., Bayas, C., Bilwes, A. M., Ortega, D. R., Falke, J. J., Zhulin, I. B., & Crane, B. R. (2013). The 3.2 A resolution structure of a receptor: CheA:CheW signaling complex defines overlapping binding sites and key residue interactions within bacterial chemosensory arrays. *Biochemistry, 52*(22), 3852-3865. doi: 10.1021/bi400383e

Liberman, L., Berg, H. C., & Sourjik, V. (2004). Effect of chemoreceptor modification on assembly and activity of the receptor-kinase complex in Escherichia coli. *Journal of Bacteriology, 186*(19), 6643-6646.

Liu, J., Hu, B., Morado, D. R., Jani, S., Manson, M. D., & Margolin, W. (2012). Molecular architecture of chemoreceptor arrays revealed by cryoelectron tomography of *Escherichia coli* minicells. *Proceedings of the National Academy of Sciences of the United States of America, 109*(23), E1481–E1488. doi: 10.1073/pnas.1200781109

Manson, M. D., Tedesco, P., Berg, H. C., Harold, F. M., & Van der Drift, C. (1977). A protonmotive force drives bacterial flagella. *PNAS, 74*(7), 3060-3064.

McEvoy, M. M., Bren, A., Eisenbach, M., & Dahlquist, F. W. (1999). Identification of the binding interfaces on CheY for two of its targets, the phosphatase CheZ and the flagellar switch protein fliM. *J Mol Biol, 289*(5), 1423-1433.

McEvoy, M. M., & Dahlquist, F. W. (1997). Phosphohistidines in bacterial signaling. *Current Opinion in Structural Biology, 7*(6), 793-797.

McEvoy, M. M., de la Cruz, A. F., & Dahlquist, F. W. (1997). Large modular proteins by NMR. *Nat Struct Biol, 4*(1), 9.

McEvoy, M. M., Hausrath, A. C., Randolph, G. B., Remington, S. J., & Dahlquist, F. W. (1998). Two binding modes reveal flexibility in kinase/response regulator interactions in the bacterial chemotaxis pathway. *PNAS, 95*(13), 7333-7338.

McNally, D. F., & Matsumura, P. (1991). Bacterial chemotaxis signaling complexes: formation of a CheA/CheW complex enhances autophosphorylation and affinity for CheY. *PNAS, 88*(14), 6269-6273.

Milburn, M. V., Prive, G. G., Milligan, D. L., Scott, W. G., Yeh, J., Jancarik, J., Koshland, D. E., Jr., & Kim, S. H. (1991). Three-dimensional structures of the ligand-binding domain of the bacterial aspartate receptor with and without a ligand. *Science, 254*(5036), 1342-1347.

Mo, G., Zhou, H., Kawamura, T., & Dahlquist, F. W. (2012). Solution structure of a complex of the histidine autokinase CheA with its substrate CheY. *Biochemistry, 51*(18), 3786-3798. doi: 10.1021/bi300147m

Morgan, D. G., Baumgartner, J. W., & Hazelbauer, G. L. (1993). Proteins antigenically related to methyl-accepting chemotaxis proteins of *Escherichia coli* detected in a wide range of bacterial species. *Journal of Bacteriology, 175*(1), 133-140.

Morrison, T. B., & Parkinson, J. S. (1997). A fragment liberated from the *Escherichia coli* CheA kinase that blocks stimulatory, but not inhibitory, chemoreceptor signaling. *Journal of Bacteriology, 179*(17), 5543-5550.

Mourey, L., Da Re, S., Pedelacq, J. D., Tolstykh, T., Faurie, C., Guillet, V., Stock, J. B., & Samama, J. P. (2001). Crystal structure of the CheA histidine phosphotransfer domain that mediates response regulator phosphorylation in bacterial chemotaxis. *Journal of Biological Chemistry, 276*(33), 31074-31082.

Ninfa, E. G., Stock, A., Mowbray, S., & Stock, J. (1991). Reconstitution of the bacterial chemotaxis signal transduction system from purified components. *Journal of Biological Chemistry, 266*(15), 9764-9770.

Pan, W., Dahlquist, F. W., & Hazelbauer, G. L. (2017). Signaling complexes control the chemotaxis kinase by altering its apparent rate constant of autophosphorylation. *Protein Science*, n/a-n/a. doi: 10.1002/pro.3179

Park, C., Dutton, D. P., & Hazelbauer, G. L. (1990). Effects of glutamines and glutamates at sites of covalent modification of a methyl-accepting transducer. *Journal of Bacteriology, 172*(12), 7179-7187.

Park, H., Saha, S. K., & Inouye, M. (1998). Two-domain reconstitution of a functional protein histidine kinase. *Proceedings of the National Academy of Sciences, 95*(12), 6728-6732.

Parkinson, J. S., Hazelbauer, G. L., & Falke, J. J. (2015). Signaling and sensory adaptation in Escherichia coli chemoreceptors: 2015 update. *Trends in Microbiology, 23*(5), 257-266.

Parkinson, J. S., & Houts, S. E. (1982). Isolation and behavior of *Escherichia coli* deletion mutants lacking chemotaxis functions. *Journal of Bacteriology, 151*(1), 106-113.

Parkinson, J. S., & Kofoid, E. C. (1992). Communication modules in bacterial signaling proteins. *Annual Review of Genetics, 26*(5102), 71-112.

Pedetta, A., Parkinson, J. S., & Studdert, C. A. (2014). Signalling-dependent interactions between the kinase-coupling protein CheW and chemoreceptors in living cells. *Molecular Microbiology, 93*(6), 1144-1155. doi: 10.1111/mmi.12727

Piasta, K. N., Ulliman, C. J., Slivka, P. F., Crane, B. R., & Falke, J. J. (2013). Defining a Key Receptor–CheA Kinase Contact and Elucidating Its Function in the Membrane-Bound Bacterial Chemosensory Array: A Disulfide Mapping and TAM-IDS Study. *Biochemistry, 52*(22), 3866-3880. doi: 10.1021/bi400385c

Prodromou, C., Roe, S. M., O'Brien, R., Ladbury, J. E., Piper, P. W., & Pearl, L. H. (1997). Identification and Structural Characterization of the ATP/ADP-Binding Site in the Hsp90 Molecular Chaperone. *Cell, 90*(1), 65-75.

Quezada, C. M., Gradinaru, C., Simon, M. I., Bilwes, A. M., & Crane, B. R. (2004). Helical shifts generate two distinct conformers in the atomic resolution structure of the CheA phosphotransferase domain from Thermotoga maritima. *J Mol Biol, 341*(5), 1283-1294. doi: 10.1016/j.jmb.2004.06.061

Quezada, C. M., Hamel, D. J., Gradinaru, C., Bilwes, A. M., Dahlquist, F. W., Crane, B. R., & Simon, M. I. (2005). Structural and chemical requirements for histidine phosphorylation by the chemotaxis kinase CheA. *Journal of Biological Chemistry, 280*(34), 30581-30585.

Sanders, D. A., Gillece-Castro, B. L., Stock, A. M., Burlingame, A. L., & Koshland, D. E., Jr. (1989). Identification of the site of phosphorylation of the chemotaxis response regulator protein, CheY. *Journal of Biological Chemistry, 264*(36), 21770-21778.

Sourjik, V., & Berg, H. C. (2002). Receptor sensitivity in bacterial chemotaxis. *Proc Natl Acad Sci U S A, 99*(1), 123-127.

Sourjik, V., & Wingreen, N. S. (2012). Responding to chemical gradients: bacterial chemotaxis. *Current Opinion in Cell Biology, 24*(2), 262-268.

Springer, W. R., & Koshland, D. E., Jr. (1977). Identification of a protein methyltransferase as the *cheR* gene product in the bacterial sensing system. *Proc Natl Acad Sci U S A, 74*(2), 533-537.

Stock, A. M., Mottonen, J. M., Stock, J. B., & Schutt, C. E. (1989). Three-dimensional structure of CheY, the response regulator of bacterial chemotaxis. *Nature, 337*(6209), 745-749.

Stock, A. M., Robinson, V. L., & Goudreau, P. N. (2000). Two-component signal transduction. *Annual Review of Biochemistry, 69*(4), 183-215.

Stock, J. B., & Surette, M. G. (1996). Chemotaxis in *Escherichia coli* and *Salmonella typhimurium*: Cellular and molecular biology. *2nd Edition (Neidhardt, F. C. et al., eds), ASM Press, Washington, D.C.*, 732-759.

Studdert, C. A., & Parkinson, J. S. (2005). Insights into the organization and dynamics of bacterial chemoreceptor clusters through *in vivo* crosslinking studies. *Proceedings of the National Academy of Sciences of the United States of America, 102*(43), 15623-15628.

Surette, M. G., Levit, M., Liu, Y., Lukat, G., Ninfa, E. G., Ninfa, A., & Stock, J. B. (1996). Dimerization is required for the activity of the protein histidine kinase CheA that mediates signal transduction in bacterial chemotaxis. *Journal of Biological Chemistry, 271*(2), 939-945.

Swanson, R. V., Alex, L. A., & Simon, M. I. (1994). Histidine and aspartate phosphorylation: two-component systems and the limits of homology. *Trends in Biochemical Sciences, 19*(11), 485-490.

Swanson, R. V., Bourret, R. B., & Simon, M. I. (1993). Intermolecular complementation of the kinase activity of CheA. *Molecular Microbiology, 8*(3), 435-441.

Swanson, R. V., Schuster, S. C., & Simon, M. I. (1993). Expression of CheA fragments which define domains encoding kinase, phosphotransfer, and CheY binding activities. *Biochemistry, 32*(30), 7623-7629.

Tanaka, T., Saha, S. K., Tomomori, C., Ishima, R., Liu, D., Tong, K. I., Park, H., Dutta, R., Qin, L., Swindells, M. B., Yamazaki, T., Ono, A. M., Kainosho, M., Inouye, M., & Ikura, M. (1998). NMR structure of the histidine kinase domain of the E. coli osmosensor EnvZ. *Nature, 396*(6706), 88-92.

Tawa, P., & Stewart, R. C. (1994). Kinetics of CheA autophosphorylation and dephosphorylation reactions. *Biochemistry, 33*(25), 7917-7924.

Toker, A. S., & Macnab, R. M. (1997). Distinct regions of bacterial flagellar switch protein FliM interact with FliG, FliN and CheY. *J Mol Biol, 273*(3), 623-634.

Tomomori, C., Tanaka, T., Dutta, R., Park, H., Saha, S. K., Zhu, Y., Ishima, R., Liu, D., Tong, K. I., Kurokawa, H., Qian, H., Inouye, M., & Ikura, M. (1999). Solution structure of the homodimeric core domain of Escherichia coli histidine kinase EnvZ. *Nat Struct Mol Biol, 6*(8), 729-734.

Vu, A., Wang, X., Zhou, H., & Dahlquist, F. W. (2012). The Receptor–CheW Binding Interface in Bacterial Chemotaxis. *Journal of Molecular Biology, 415*(4), 759-767.

Wadhams, G. H., & Armitage, J. P. (2004). Making sense of it all: bacterial chemotaxis. *Nat. Rev. Mol. Cell Biol., 5*(12), 1024-1037.

Wang, X., Vu, A., Lee, K., & Dahlquist, F. W. (2012). CheA–receptor interaction sites in bacterial chemotaxis. *Journal of Molecular Biology, 422*(2), 282-290.

Welch, M., Chinardet, N., Mourey, L., Birck, C., & Samama, J.-P. (1998). Structure of the CheY-binding domain of histidine kinase CheA in complex with CheY. *Nature Structural Biology, 5*, 25 - 29.

Welch, M., Oosawa, K., Aizawa, S., & Eisenbach, M. (1993). Phosphorylation-dependent binding of a signal molecule to the flagellar switch of bacteria. *Proc Natl Acad Sci U S A, 90*(19), 8787-8791.

West, A. H., & Stock, A. M. (2001). Histidine kinases and response regulator proteins in two-component signaling systems. *Trends in Biochemical Sciences, 26*(6), 369-376.

Wigley, D. B., Davies, G. J., Dodson, E. J., Maxwell, A., & Dodson, G. (1991). Crystal structure of an N-terminal fragment of the DNA gyrase B protein. *Nature, 351*(6328), 624-629.

Williamson, M. (2012). How Proteins Work. *Garland Science, United States*, pp 130.

Wolanin, P., Thomason, P., & Stock, J. (2002). Histidine protein kinases: key signal transducers outside the animal kingdom. *Genome Biology, 3*(10), 3013.3011-3013.3018.

Wylie, D., Stock, A., Wong, C. Y., & Stock, J. (1988). Sensory transduction in bacterial chemotaxis involves phosphotransfer between Che proteins. *Biochem Biophys Res Commun, 151*(2), 891-896.

Yaginuma, H., Kawai, S., Tabata, K. V., Tomiyama, K., Kakizuka, A., Komatsuzaki, T., Noji, H., & Imamura, H. (2014). Diversity in ATP concentrations in a single bacterial cell population revealed by quantitative single-cell imaging. *Scientific Reports, 4*, 6522.

Yeh, J. I., Biemann, H. P., Prive, G. G., Pandit, J., Koshland, D. E., Jr., & Kim, S. H. (1996). High-resolution structures of the ligand binding domain of the wild- type bacterial aspartate receptor. *J Mol Biol, 262*(2), 186-201.

Zhang, J., Xu, Y., Shen, J., Luo, X., Chen, J., Chen, K., Zhu, W., & Jiang, H. (2005). Dynamic Mechanism for the Autophosphorylation of CheA Histidine Kinase: Molecular Dynamics Simulations. *Journal of the American Chemical Society, 127*(33), 11709-11719.

Zhao, R., Collins, E. J., Bourret, R. B., & Silversmith, R. E. (2002). Structure and catalytic mechanism of the *E. coli* chemotaxis phosphatase CheZ. *Nat Struct Biol, 9*(8), 570-575.

Zhu, Y., Qin, L., Yoshida, T., & Inouye, M. (2000). Phosphatase activity of histidine kinase EnvZ without kinase catalytic domain. *Proceedings of the National Academy of Sciences, 97*(14), 7808-7813.

Zhulin, I. B. (2001). The superfamily of chemotaxis transducers: From physiology to genomics and back. *Advances in Microbial Physiology, 45*, 157-198.

VITA

Wenlin Pan was born on July 2, 1989, in Changchun, China. He received his Bachelor's degree in Biotechnology from Jilin University in 2012. He was enrolled in the PhD program of Biochemistry Department in the University of Missouri – Columbia in 2012. He started working under the supervision of Dr. Gerald L. Hazelbauer in 2013. Wenlin completed his Doctorate of Philosophy in Biochemistry from the University of Missouri - Columbia in July, 2017.